# DECADAL DYNAMICS OF NIGHTTIME URBAN HEAT ISLAND IN COIMBATORE: A SPATIO-TEMPORAL INVESTIGATION OF THERMAL CLUSTERING AND INTENSIFICATION

KAJESH GADEKAR[1], ANEESH MATHEW [2*], SARWESH P[3], CHINTHU NARESH[4]

*[1,4]Research Scholar, Department of Civil Engineering, National Institute of Technology, Tiruchirappalli, 620015, Tamil Nadu, India*
*[2]Assistant Professor, Department of Civil Engineering, National Institute of Technology, Tiruchirappalli, 620015, Tamil Nadu, India*
*[3]Associate Professor, School of Computer Science and Engineering, Vellore Institute of Technology, Vellore, 632014, Tamil Nadu, India*
**Corresponding author email: aneesh52006@gmail.com; aneesh@nitt.edu*

**Received:** 1st July 2025, **Accepted:** 10th November 2025

## ABSTRACT

This study presents a comprehensive spatio-temporal analysis of nighttime Land Surface Temperature (LST) and Urban Heat Island Intensity (UHII) in Coimbatore from 2001 to 2022, highlighting statistically significant warming trends and intensifying urban heat island effects. Urban areas experienced a notable nighttime LST increase from 21.4 °C in 2001 to 23.7 °C in 2019, compared to a rural rise from 20.5 °C to 22.5 °C. The average urban–rural LST differential (~1 °C) widened post-2016, aligning with the recorded peak LST of 26.8 °C. The minimum LST dropped to 8.5 °C in 2001, indicating a reduction in cold extremes. Kendall's tau analysis confirmed a stronger warming trend in urban areas ($\tau$ = 0.593) than rural zones ($\tau$ = 0.429). Seasonal UHII analysis showed progressive winter intensification post-2012, while summer UHII peaked in 2013 and 2015, then dipped post-2016 before rising again in 2022. Mann-Kendall tests confirmed statistically significant increasing trends in winter UHII, urban LST, and rural LST, with urban LST exhibiting the steepest rise. Spatial autocorrelation analysis using Moran's Index revealed intensifying clustering of high LST zones: the annual Moran's Index increased from 0.797 (2001) to 0.857 (2022), with z-scores rising from 42.253 to 45.445. Winter showed the most pronounced clustering, with Moran's Index jumping from 0.812 to 0.903 and z-scores reaching 47.848 by 2022. Hotspots with 99 % confidence levels were primarily urban, expanding over time with temperatures between 24.8 °C and 26.7 °C, while cold spots (99 % CL) remained stable in rural areas. These findings confirm the persistent and intensifying nature of UHI in Coimbatore, driven by urban expansion, declining vegetation, and increased impervious surfaces. This study fills a critical research gap by providing one of the first long-term assessments of nighttime UHI intensity in a mid-sized Indian city, thereby contributing to the broader understanding of urban thermal dynamics beyond metropolitan regions. The study underscores the urgent need for spatially informed interventions, such as urban greening, reflective materials, and climate-sensitive planning, to mitigate urban thermal stress and enhance resilience in rapidly growing cities.

**Keywords**: Urban Heat Island (UHI); Land Surface Temperature (LST); Thermal Hotspots; Mann-Kendall Trend Test; Climate Mitigation Strategies

## INTRODUCTION

Rapid urbanization has profoundly transformed local temperatures, with the Urban Heat Island (UHI) effect becoming a significant environmental issue. UHI refers to the temperature disparity between urban and rural areas, primarily driven by anthropogenic activities, land cover changes, and reduced vegetation (Arunab & Mathew, 2024). This phenomenon intensifies thermal discomfort, increases energy demands, and exacerbates public health risks, particularly during extreme heat events. While numerous studies have explored UHI dynamics in major global cities, research on Indian coastal cities like Coimbatore remains limited despite their unique climatic and geographic conditions. Human and environmental factors combine to cause UHI, a phenomenon that causes significantly higher temperatures in metropolitan or urban areas compared to nearby rural areas (Gupta *et al*., 2020; Khandelwal *et al*., 2018). UHI intensity is typically more pronounced at night and during calm weather, owing to greater surface heat retention in impervious materials (Mathew *et al*., 2018). Rapid urbanization and population growth have significantly altered land use and land cover (LULC) in developing nations, replacing natural vegetation and permeable soils with impervious materials such as asphalt and concrete. These surfaces absorb and retain heat, disrupting surface energy balance and elevating urban temperatures (Oke, 1982; Voogt & Oke, 2003; Voogt, 2007; Mohan *et al*., 2013; Mahata *et al*., 2024; Grimm *et al*., 2008). This environmental issue results from the replacement of natural vegetation with impervious surfaces such as concrete and asphalt, which absorb and retain heat, causing elevated temperatures in urban centers compared to surrounding rural areas. The UHI effect exacerbates urban environmental challenges, including increased energy consumption, deteriorating air quality, and heightened heat stress, particularly during extreme heat events (Rizwan *et al*., 2008; Badugu *et al*., 2023).

UHIs have profound implications for human health, particularly in rapidly urbanizing regions. Elevated temperatures within urban areas intensify heat stress and contribute to increased incidences of cardiovascular and respiratory illnesses (Tong *et al*., 2021; Mora *et al*., 2017). During extreme heat events, UHIs can significantly amplify mortality rates, especially among vulnerable populations such as the elderly, children, and outdoor workers (Harlan *et al*., 2006). Aghazadeh *et al*. (2025) have noticed that heat waves combined with strong SUHI effects significantly reduce thermal comfort in Tabriz, Iran, particularly for children, the elderly, and adult females in nine high-risk areas. Furthermore, higher urban temperatures accelerate photochemical reactions, increasing ground-level ozone and fine particulate matter concentrations, thereby compounding respiratory risks (Tan *et al*., 2010; Arunab & Mathew, 2024). These combined thermal and air-quality stressors pose serious challenges to public health and urban sustainability. Therefore, assessing the spatiotemporal dynamics of UHIs is not only crucial for understanding urban climate variability but also for formulating effective heat adaptation and mitigation strategies that safeguard human health. UHIs are a growing concern, often linked to a decline in air and water quality compared to surrounding rural areas. This phenomenon has spurred scientists to urge proactive measures from both urban residents and architects in mitigating its effects. Human activities and transportation systems such as vehicles, buses, and trains generate concentrated energy, which significantly raises temperatures in major cities like New York, Paris, and London (Hua *et al*., 2020). The spatiotemporal relationship between urban green development and the UHI effect is critical for achieving balanced urban development (Liu & Zhang, 2025). Recognizing the adverse impacts of UHIs, it is vital to adopt proactive strategies for sustainable urban living. Promoting responsible development can foster healthier cities that balance economic growth with environmental well-being and improved quality of life.

Pandey *et al*. (2024) have observed that the seasonal relationship between land surface temperature (LST) and various vegetation indices, as well as land surface indices, exhibits distinct patterns depending on the season and urban land cover. Shahfahad *et al*. (2021) observed that metropolitan areas contain more impermeable surfaces, such as concrete, glass, and metal, which absorb and reflect heat, increasing LST. Urban hotspots are high LST surfaces with intense temperature conditions. To mitigate temperature and maintain urban ecosystems, these UHS must be identified and monitored. Mathew *et al*. (2017) examined how UHI affected development, vegetation, and elevation in Jaipur spatially and seasonally. This study examined the UHI effect in Jaipur, India, throughout summer, monsoon, and winter utilizing eight days of mean nighttime LST data. Significant SUHI was found in 13 years of LST data from 2003 to 2015. Zwolska *et al*. (2025) observed that land use and land cover changes significantly increased SUHI intensity in Poznań, Poland, over 33 years. Built-up areas expanded by 7.4 %, and hot island areas grew by 5.6 km², mainly in industrial and compact mid-rise zones. SUHI peaks shifted from spring to autumn, with temperature rises of up to +2.8 °C in spring and +2.5 °C in summer, while some residential areas cooled by –0.9 °C. The study highlights the need for climate-sensitive urban planning. Hao *et al*. (2025) have observed that incorporating dynamic urban boundaries in UHI measurements is crucial for accurately assessing the impact of urbanization on heat-related risks. Their study, using data from 2000 to 2015, reveals a 10 % increase in global SUHI intensity, with newly built-up areas experiencing a 0.61 °C rise in summer UHI intensity. This warming contributes to a 20 % increase in summer heat-related risks and mortality, affecting over 2.3 % of the global population.

Kara *et al*. (2025) found that urbanization intensified SUHI effects in Samsun, Türkiye, from 2014 to 2023. Built-up areas warmed from ~25 °C to over 31 °C, while water bodies stayed below 23 °C. Vegetated areas were 7–8 °C cooler than urban zones, with differences reaching 12 °C in industrial areas, underscoring the strong impact of land cover changes on urban heat. Patriota *et al*. (2024) observed that urbanization intensified UHI intensity in 21 Brazilian metropolitan regions (2003–2022), with daytime UHI intensity 60 % (1.64 °C) higher than nighttime. Urban expansion drove daytime LST. Evapotranspiration mitigated daytime LST, whereas nighttime LST was influenced by net surface radiation, increasing sensible heat availability. Lopes & Hora (2024) have noticed that urban morphology significantly influences UHI intensity, particularly through factors like urban canyons and the height-to-width ratio of streets. Raj & Yun (2025) have noticed that summer daytime SUHI intensity has declined in Seoul but increased in Ulsan, South Korea, from 2001 to 2022. In Seoul, SUHI decreased by −0.03 °C/yr (Terra) and −0.05 °C/yr (Aqua), linked to rising vegetation, while Ulsan experienced an increase of +0.04°C/yr due to vegetation loss. Peak SUHI values reached 2.98 °C in Seoul and 3.39 °C in Ulsan during June, highlighting that urban greenery expansion effectively mitigates heat stress and supports sustainable city planning. Puttanapong *et al*. (2025) found that urbanization in Bangkok intensified the SUHI effect, rising from 3 °C to 4.8 °C before easing to 4.1 °C due to greening efforts. Green and blue infrastructure helped reduce heat, while economic and policy shifts shaped land use. Kim *et al*. (2025) have found that integrating high-rise buildings with green spaces significantly enhances urban cooling and reduces energy consumption. Their ENVI-met simulations in a Seoul urban renewal area showed a 0.94 °C decrease in mean air temperature and a 1.80 % reduction in energy use. Peng *et al*. (2024) have observed that seasonal changes in rural landscapes significantly influence UHI intensity variations. Their findings emphasize the need for refined rural reference landscape descriptions and city-specific UHI intensity evaluation thresholds to enhance result interpretability and comparability.

Several studies have explored UHI effects globally and regionally, providing insights into the spatial variation and intensity of the phenomenon. For example, Peng *et al*. (2012) conducted a global analysis of UHI intensity across major cities using satellite-derived temperature data, highlighting the critical role of urbanization patterns in shaping thermal anomalies. In India, Sharma & Joshi (2013) studied UHI patterns in major Indian cities, emphasizing how varying LULC dynamics contribute to the intensity and spatial distribution of surface temperatures. Similarly, Ramachandra *et al*. (2019) demonstrated how increased built-up areas in Indian metropolitan regions have led to intensified UHI effects, underscoring the necessity of green infrastructure interventions. While urbanization has improved many areas of human existence, it has also created new environmental problems, including air pollution, global warming, and environmental degradation because of how convenient and high-quality urban living is. Over five billion people are predicted to live in metropolitan regions by 2030, signalling an acceleration of the urbanization trend (Mathew *et al.,* 2024). As global warming intensifies, nearly 30 % of the global population lives in areas where temperatures exceed life-threatening thresholds for at least 20 days each year. However, the distribution of heat and vulnerability differs across urban areas, presenting a critical question (Wang & Chang, 2020). Radoux *et al*. (2025) found that built-up areas are about 8.9 °C warmer than the city average, while broadleaf trees are 7.4 °C cooler. Using high-resolution Landsat-8 data, they showed that urban green spaces effectively reduce SUHI intensity and stressed the need for better night-time temperature monitoring to capture full heat dynamics. Urban area growth is a major environmental concern due to the hazards that large-scale population migration to urban regions poses to land areas (Mathew *et al*., 2018). Thus, it is essential to carry out research on the UHI in order to influence future urban growth and planning, especially in developing countries such as India. In-depth research on UHI effects empowers policymakers and urban planners to make well-informed decisions, addressing the challenges presented by rapid urbanization and ensuring sustainable urban growth.

Satellite-based thermal infrared data and LULC classification enable the detection of surface temperature variations and the quantification of urban-induced thermal anomalies (Li *et al*., 2017). Wang *et al*. (2025a) found that UHIs in the Central-Southern Liaoning Urban Agglomeration expanded from 2013 to 2020, with urban cores acting as thermal hubs spreading heat across boundaries. Vegetation cooled locally but showed indirect warming effects nearby, while population density increased and GDP reduced UHI impacts. They highlight the need for regional, not city-level, heat mitigation planning. Grigoraș & Urițescu (2018) investigated the relationship between LST and air temperature in Bucharest using MODIS satellite data and weather station records. The study found higher correlation coefficients during nighttime (0.8-0.87) compared to daytime (0.71-0.77). Additionally, Getis-Ord spatial analysis identified "very hot" zones primarily concentrated in the city center, along major streets, and in densely populated areas. These zones accounted for 33.2 % of the area during the day and 31.6 % at night, with a stable central "very hot" zone covering 27.1 % throughout the study period. Arunab & Mathew (2023) observed that the effects of urban heat islands in Bangalore and Hyderabad have intensified because of urbanization and human activities. Analysis of two decades of MODIS LST data revealed average UHI intensities of 1.9 °C in Bangalore and 2.44 °C in Hyderabad, with annual increments of 0.040 °C and 0.033 °C, respectively. The research underscores the necessity for focused UHI mitigation initiatives, emphasizing the most at-risk areas. Pandey *et al*. (2014) observed that UHI formation in Delhi is influenced by aerosol load and land-cover variations. Temperatures in Delhi are higher than in surrounding areas, especially at night,

with nocturnal UHI intensity ranging from 0–2 K during the monsoon and peaking at 4–6 K in March. Spatial analysis showed that aerosol optical depth (AOD), along with land-cover factors like built-up areas and vegetation, plays a key role in UHI formation, while thermal inertia also affects the urban-rural thermal structure.

Despite extensive global research, there is a notable gap in comprehensive UHI studies focusing on Tamil Nadu's fast-growing cities. Prior studies have largely focused on megacities like Delhi and Mumbai, leaving mid-sized cities such as Coimbatore underexplored in terms of spatio-temporal UHI dynamics. Although numerous studies have explored UHI dynamics in India, most have concentrated on major metropolitan centers such as Delhi, Mumbai, Bengaluru, and Hyderabad (Arunab & Mathew, 2023; Pandey *et al*., 2014; Grover & Singh, 2015; Shahfahad *et al*., 2021). However, mid-sized Tier-2 cities like Coimbatore remain relatively underexplored, despite experiencing rapid industrialization, population growth, and unplanned land-use transitions that significantly alter local thermal environments. The lack of long-term, high-resolution analyses in such cities limits the understanding of how secondary urban centers contribute to regional heat stress and climate vulnerability. Therefore, this study bridges this gap by conducting a two-decade (2001–2022) assessment of nighttime LST and UHI intensity in Coimbatore, integrating statistical trend tests and spatial autocorrelation analysis to uncover evolving heat patterns and their implications for urban resilience. Addressing this gap can help develop targeted adaptation strategies for cities facing diverse climatic challenges. The novelty of this work lies in its integration of trend detection and spatial autocorrelation techniques to identify statistically significant warming patterns and thermal clustering. The study aims to examine long-term changes in nighttime LST and UHII, evaluate spatial clustering of heat zones, and propose mitigation strategies aligned with climate-resilient urban planning. By focusing on a mid-sized Indian city, this research advances understanding of UHI dynamics beyond megacities and provides valuable insights for evidence-based urban heat management. Tamil Nadu, a rapidly urbanizing state in southern India, has experienced significant urban expansion in recent decades. Among its major cities, Coimbatore stands out due to its socio-economic prominence and contrasting climatic conditions. Coimbatore, located inland near the Western Ghats, experiences a more moderate climate. These contrasting geographical and climatic settings provide an ideal context for analyzing the spatial and temporal dynamics of the UHI effect. Halder *et al*. (2024) have observed that the rapid urbanization in Bhubaneswar has led to significant alterations in land use and land cover, contributing to the intensification of seasonal urban heat islands. The study highlights that the expansion of built-up areas, coupled with a notable reduction in vegetation cover, has exacerbated the UHI effect, particularly during summer and winter. These modifications highlight the essential requirement for sustainable urban development strategies to alleviate heat island phenomena and tackle the related environmental issues.

Coimbatore, a rapidly expanding metropolitan city in southern India, experiences significant UHI impacts due to its high population density, extensive built-up areas, and limited green cover. Situated near the Western Ghats, the city's inland setting and unique topography influence its local thermal environment, making it an ideal case study for assessing UHI dynamics in rapidly urbanizing regions. Previous research has often focused on short-term LST trends or seasonal patterns, leaving gaps in understanding the long-term spatiotemporal variability of UHI intensity in such complex environments. This study addresses these gaps by employing robust statistical methods, including the Mann-Kendall trend test and Kendall's τ analysis, to assess LST trends and UHI intensity over time. The study also investigates the seasonal variability of UHI intensity, emphasizing how winter and summer months respond differently to urban heating processes. The novelty of this study lies

in its comprehensive temporal analysis, integrating long-term LST records and statistical trend evaluation to capture UHI variations in the city. By linking observed UHI patterns to potential mitigation strategies, this research provides a foundation for sustainable urban planning tailored to tropical cities. The findings contribute to a deeper understanding of UHI dynamics in underexplored regions, offering valuable insights for policymakers, urban planners, and climate researchers aiming to build climate-resilient urban environments. Despite extensive global research, there is a notable gap in comprehensive UHI studies focusing on Tamil Nadu's fast-growing cities. This study aims to assess the spatio-temporal dynamics of the UHI effect in Coimbatore using geospatial techniques. The research evaluates surface temperature patterns and their relationships over time, contributing to the development of targeted urban planning and climate resilience strategies. By addressing the UHI phenomenon in the rapidly developing city, the study seeks to inform sustainable urban development policies tailored to diverse climatic and geographic settings in Tamil Nadu.

## STUDY AREA

The Coimbatore City Corporation stands as a pivotal industrial center in the state of Tamil Nadu, India. Serving as the headquarters of Coimbatore District, it evolved from a municipality established in 1866, initially accommodating a population of 24,000 within a spatial extent of 10.88 $km^2$. The study area spans latitudes 10° 54′ 45″N to 11° 6′ 15″N and longitudes 76° 52′ 10″E to 77° 3′ 55″E, covering an expansive 260.8 $km^2$, inclusive of surface water bodies. As per the 2001 Census, the population of Coimbatore City was 9.3 lakh, marking a steady increase from 0.47 lakh in 1911. This reflects an average annual growth rate of 2.7 % and an average decadal growth rate of 27.34 %, highlighting the city's consistent demographic expansion over the past century (CCMC, 2006). The population of Coimbatore was approximately 10.2 lakh (Census of India, 2011). Notably, in 2012, the city underwent significant expansion as the corporation city boundary was redrawn, amalgamating nearby areas and villages into the Coimbatore City Corporation (CCMC). Consequently, the city's area more than doubled, increasing from 105.6 $km^2$ to its current extent. Climatically, Coimbatore experiences a tropical savanna climate (Aw) under the Köppen–Geiger classification (Peel *et al*., 2007), characterized by distinct wet and dry seasons. The city receives moderate rainfall primarily during the southwest monsoon (June–September) and the northeast monsoon (October–December), with an average annual precipitation of about 600–700 mm. The mean annual temperature ranges between 24 °C and 32 °C, with April and May being the hottest months. The surrounding Western Ghats play a crucial role in moderating the city's temperature and influencing its rainfall distribution (Ramanathan & Kokilavani, 2021). Fig. 1 displays the study area's geographic location.

**Fig. 1: Geographical location of Coimbatore study area**

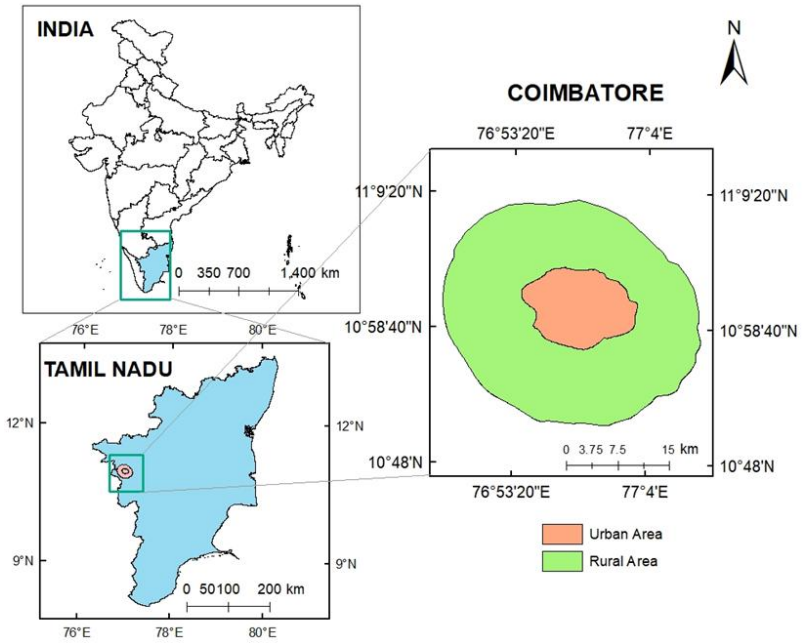


## DATA AND METHODOLOGY

A meticulous examination is conducted to unravel the temporal and spatial variations of the UHI phenomenon over the city of Coimbatore. This involves a thorough analysis of UHI patterns, with a specific focus on identifying trends in summer and winter seasons. The study extends to the identification of zones within the study area that exhibit thermal discomfort. Fig. 2 shows the flowchart of methodology.

**Fig. 2: Flowchart of methodology**

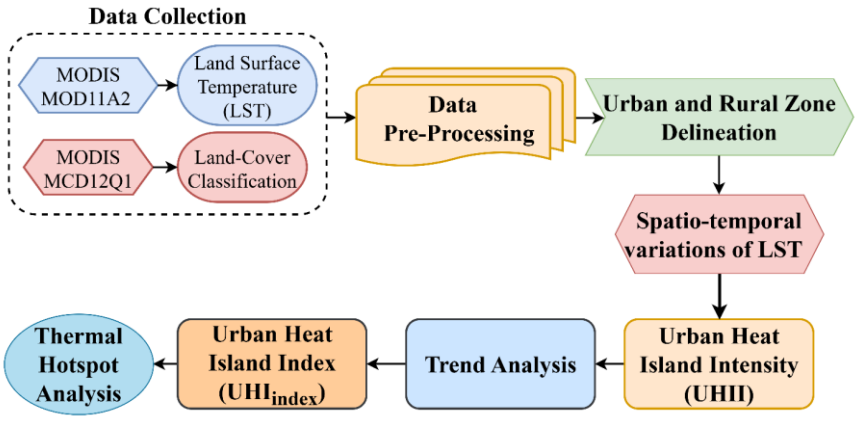

MODIS is a platform-based sensor that uses 36 wavebands to collect data on the Earth's surface. These wavebands include thermal, visible, near-infrared (NIR), and short-wave infrared (SWIR) spectra. For MODIS products, a range of processing levels and temporal resolutions are available, including daily, eight-day, sixteen-day, monthly, quarterly, and annual (Badugu *et al*., 2023; Xiong *et al*., 2020).

**Table 1: Details of MODIS products utilized in the study**

| Dataset/Product | Source/Platform | Variables | Spatial Resolution | Temporal Resolution | Data Format | Application/Purpose in Study |
|---|---|---|---|---|---|---|
| **MOD11A2** | MODIS, Terra Satellite (NASA LP DAAC) | Land Surface Temperature (LST, °C) | 1 km | 8-day composite | HDF | Estimation of LST, computation of Surface Urban Heat Island (SUHI) intensity, and trend analysis |
| **MCD12Q1** | MODIS, Terra & Aqua Combined Product (NASA LP DAAC) | Land Cover Type (IGBP classification scheme) | 500 m | Annual | HDF | Identification of urban and non-urban classes |

The study employed two key MODIS products—MOD11A2 and MCD12Q1—obtained from the NASA Land Processes Distributed Active Archive Center (LP DAAC). The MOD11A2 product provides 8-day composite Land Surface Temperature (LST) data at a spatial resolution of 1 km (Wan *et al*., 2015), enabling the estimation of seasonal and annual LST variations and the computation of Surface Urban Heat Island (SUHI) intensity over the study period. The MCD12Q1 product, derived from combined Terra and Aqua MODIS observations, offers annual global land cover classification at 500 m resolution following the International Geosphere–Biosphere Programme (IGBP) scheme (Friedl *et al*., 2010). This dataset was used to delineate urban and non-urban areas, facilitating the analysis of thermal contrasts and the assessment of urban expansion impacts. Together, these satellite products provided consistent, long-term, and spatially detailed information for examining the spatiotemporal dynamics of urban thermal environments and their linkage with land use/land cover transitions in Coimbatore.

**Urban Heat Island Intensity**

The temperature differential between urban centres and the rural or suburban areas that surround them is referred to as UHI intensity. According to Badugu *et al*. (2023), the heat island effect measures the degree to which metropolitan regions are noticeably warmer than their surrounding non-urban areas. Understanding the effects of urbanization on regional climates and evaluating the possible dangers associated with heat in urban settings require an understanding of UHI intensity. It can support the creation of urban heat management policies, mitigation plans, and urban planning.

UHI intensity is estimated by subtracting rural or reference area temperatures from urban temperatures. This temperature difference shows that urban activities and the environment

promote heat retention and generation (Mathew *et al*., 2016; Wang *et al*., 2023). The latter must be carefully selected. The non-urban site should be near a city yet rural or have lots of natural greenery. The temperature differential between urban and rural areas is used to measure UHI intensity, as shown in equation 1. The term "rural" used to refer to a non-urban location.

$$\text{UHI Intensity (UHII)} = LST_{Urban} - LST_{Rural} \quad (1)$$

Where, $LST_{Urban}$ is the LST of the urban region and $LST_{Rural}$ is the LST of the nearby rural region.

**Urban Heat Island Index**

Numerous studies have demonstrated that the most important aspect to look at in any analysis of UHI effects is the absolute magnitude of UHI intensity (Dewan *et al*., 2021; Mathew *et al*., 2016; Wang *et al*., 2023). The maximum and lowest temperature measurements in the research zone typically occur at different locations. These spots are scattered throughout the research area; it doesn't matter where they are precisely. Every site experiences significant variation in temperature throughout the year. Because seasonal and diurnal variations in the temperature range might affect the UHI intensity across a study region, it is possible that it will not remain consistent over time. The difference between the greatest and least LST values measured inside the research area can be used to calculate the SUHI intensity over a city using its thermal infrared image. Comparing UHI intensity over time is difficult, though, because of the varying intensity of UHI and the shift or change in the positions corresponding to the maximum and minimum LST values. This also prevents comparing the UHI effects of different cities over time (Mathew *et al*., 2016; Mohammad & Goswami, 2021).

Furthermore, it is unable to combine and analyze the UHI effect across the research area utilizing disparate perspectives on LST data. The UHI index application was created to make it easier to examine the UHI effect in greater depth using a large number of photographs. The $UHI_{index}$ is derived using equation 2 and the LST values detected in any image (Mathew *et al*., 2016).

$$UHI_{index} = \frac{(LST_i - LST_{min})}{(LST_{max} - LST_{min})} \quad (2)$$

LST, or the location/pixel of the study region, is the source of $UHI_{index}$. after examining the identical picture that $LST_i$ was taken from. The locations/pixels in the research region that exhibit the highest and lowest LSTs are designated as $LST_{max}$ and $LST_{min}$. The $UHI_{index}$ for each pixel in the research region that corresponds to an image may be determined using this method. Since the $UHI_{index}$ is a normalized index with only 0 and 1 values, it can be used to compare the severity of UHI over various time periods and seasons. Through normalization (between zero and one), the $UHI_{index}$ was utilized to bring the varied LST range (and consequently the UHI intensity) into a regular range. This range, rather than the actual UHI intensity, illustrates the relative UHI effect in various city (research area) segments. This method helps to mitigate the impact of notable occurrences observed for whatever reason, which facilitates the analysis of both seasonal and long-term effects, as tried in this work. We used the $UHI_{index}$ to pinpoint hotspot locations.

**Trend Analysis**

The Mann-Kendall test is a non-parametric statistical tool employed to analyze time series data and determine the statistical significance of a monotonic trend (Kendall, 1938). The present study used the Theil-Sen slope estimator (Sen, 1968) to ascertain the slope (magnitude) of the trend and utilizes the Mann-Kendall test to evaluate whether the LST and UHI intensity are exhibiting an upward or downward trend.

**Mann-Kendall Test**

The Mann-Kendall test, developed by Mann & Kendall in 1945 and 1975, respectively, is a widely used rank-based, non-parametric statistical test for detecting trends in time series data. It is particularly useful in analyzing environmental and climatological data where the assumptions of normality and linearity may not hold. The test assesses whether there is a monotonic trend (either increasing or decreasing) present in a dataset over time, without making assumptions about the distribution of the data (Mahajan & Dodamani 2015; Das *et al*., 2019; Aher & Yadav 2021).

The test evaluates whether a consistent upward or downward trend exists in data without requiring it to follow any specific distribution. The test statistic S of the time series $X_1$, $X_2$, $X_3$…. $X_n$ is calculated from equation 3.

$$\text{The Mann-Kendall test static (S)} = \sum_{j=1}^{n-1} \sum_{k=j+1}^{n} \text{sgn}(x_k - x_j) \quad (3)$$

Where the sgn $(x_k - x_j)$ are calculated using equation 4,

$$Sgn\ (x_k - x_j) = \begin{cases} 1, & \text{if } (x_k - x_j) > 0 \\ 0, & \text{if } (x_k - x_j) = 0 \\ -1, & \text{if } (x_k - x_j) < 0 \end{cases} \quad (4)$$

In equation (4), $x_k$ and $x_j$ are the data values in the time series at time steps k and j, where k >j. The variance of S is computed from equation 5.

$$\text{The variance, Var(S)} = \frac{n(n-1)\ (2n+5)}{18} \quad (5)$$

Kendall's Tau measures the strength of the monotonic trend and is computed as in equation 6.

$$\tau = \frac{S}{\frac{1}{2}n(n-1)} \quad (6)$$

Here n represents the number of data in the observations.

The Sen's slope and the intercept of the line fitted through a data are calculated using the equations of 7 and 8.

$$\text{Sen's slope } \beta = \text{median } \left[\frac{x_k - x_j}{k-j}\right] \quad (7)$$

$$\text{The slope intercept} = \bar{x} - \beta(\bar{t}) \quad (8)$$

The $\bar{x}$, $\bar{t}$ represents the mean of the data and time period.

The significance level (p) determines whether the detected trend is statistically significant or not. To test the null hypothesis ($H_0$) of no trend against the alternative hypothesis ($H_a$) of the presence of a trend at a 0.05 level of significance ($\alpha = 0.05$), $H_0$ is rejected if the p-value is less than 0.05. A positive $\tau$ value indicates an increasing trend, whereas a negative $\tau$ value indicates a decreasing trend.

The MK test identifies only the direction of the trend. Therefore, the magnitude of the trend was determined using the Theil–Sen estimator, which provides a robust estimate of the rate of change. All these computations including Kendall's Tau ($\tau$), p-value, and Sen slope, were determined using the R -programming language.

**Hotspot Analysis**

However, hotspots can be identified by their pixel LST value; in this case, the significance of that specific pixel is determined by the influence of its neighboring pixels on the hotspot analysis. Here, the obtained raster set is transformed into a point data set and incorporated into the study's input feature class.

The Hot Spot Analysis tool dataset's Getis-Ord Gi* statistic is computed for every feature. The z-scores and p-values of the outcome show the regional clustering of qualities with high or low values (Rossi & Becker, 2019). This tool functions by examining each feature in light of its surrounding environment. A high-value feature may not indicate a statistically significant hotspot, despite its fascinating nature. A characteristic must have a high value and should also be surrounded by additional high values in order to be considered statistically significant. A feature's local sum and the sums of its neighbors are compared proportionately to the total of all features. A feature's local sum and the sums of its neighbors are compared proportionately to the total of all features (Ord & Getis, 1995).

The Getis-Ord local statistic is given as,

$$G_i^* = \frac{\sum_{j=1}^{n} w_{i,j} X_j - \bar{X} \sum_{j=1}^{n} w_{i,j}}{S \sqrt{\frac{\left[ n \sum_{j=1}^{n} w_{i,j}^2 - \left( \sum_{j=1}^{n} w_{i,j} \right)^2 \right]}{n-1}}} \quad (9)$$

Where $X_j$ is the attribute value for feature j, $W_{i,j}$ is the spatial weight between features i and j, n is equal to the total number of features and

$$\bar{X} = \frac{\sum_{j=1}^{n} X_j}{\mathrm{n}} \quad (10)$$

$$S = \sqrt{\frac{\sum_{j=1}^{n} X_j^2}{n} - (\bar{X})^2} \quad (11)$$

The Gi statistic is a z score, so there is no need for further calculations.

The methodological framework employs spatial metrics such as inverse Euclidean distance and maximum neighbor distance, taking into account only the eight immediate neighboring pixels for analysis (Mavrakou *et al*., 2018; Guerri *et al*., 2021; Badugu *et al*., 2023). For every feature in the input feature class, this tool creates a new output feature class that includes the feature's z-score, p-value, and confidence level bin (Gi Bin). If a selection set is added to the input feature class, just those features will be inspected, and the output feature class will only display those features (Ord & Getis, 1995).

**Spatial Auto-correlation**

According to Waldo Tobler's First Law of Geography, "everything is related to everything else, but near things are more related than distant things." Spatial autocorrelation provides a fundamental basis for understanding spatial relationships; however, perfect autocorrelation is extremely rare and must be carefully considered during spatial analysis. It describes how data values are related to themselves in space and helps determine whether spatial patterns exhibit positive or negative correlation.

Spatial autocorrelation is commonly measured using **Moran's I index**, which can indicate **positive**, **negative**, or **zero** spatial correlation. A positive Moran's I value signifies that similar values cluster together, while a negative value indicates spatial dispersion. A value near zero suggests a random spatial distribution. **Fig. 3** illustrates these clustering patterns (Chen, 2021).

The **null hypothesis ($H_0$)** states that there is no spatial autocorrelation among the observed elements. The **z-score** and **p-value** indicate the statistical significance of the observed pattern, while **Moran's I** reflects the direction and degree of spatial association. If the *p*-value is small, it implies that the observed spatial pattern is highly unlikely to have occurred by random chance.

**Fig. 3: Different clustering patterns**

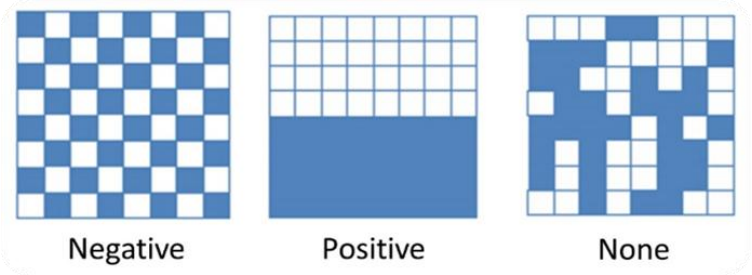


Discovered hotspots or cold zones are considered statistically significant if the probability value is low and the Z absolute value is significant (Ord & Getis, 1995). The Getis-Ord Index and significance levels classification have been shown in Table 2.

**Table 2: Getis-Ord Index and Significance levels classification**

| p-Value | Z-Score | GI index | Significance |
|---|---|---|---|
| -0.01 | < -2.58 | -3 | 99% confident Cold-Spot |
| -0.05 | -2.58 to -1.96 | -2 | 95 % confident Cold-Spot |
| -0.1 | -1.96 to -1.65 | -1 | 90 % confident Cold-Spot |
| ------ | -1.65 to 1.65 | 0 | Random |
| 0.1 | 1.65 to 1.96 | 1 | 90 % confident Hot-Spot |
| 0.05 | 1.96 to 2.58 | 2 | 95 % confident Hot-Spot |
| 0.01 | > 2.58 | 3 | 99 % confident Hot-Spot |

## RESULTS AND DISCUSSION

### Land Surface Temperature

Over a span of twenty-two years (2001-2022), a comprehensive examination of nighttime LST in the city of Coimbatore was undertaken, specifically concentrating on the winter and summer. The analysis uncovered noticeable temperature variations within the urban and rural perimeters. Notably, the central areas of the city displayed elevated temperatures in contrast to the surrounding locales. The temperatures near these central regions were moderate, recording lower values than those in the central zones.

For Coimbatore, the average yearly LST as well as the average LST throughout the summer and winter are depicted in Fig. 4, along with their temporal and spatial fluctuations. In 2001, the urban center had the highest LST, and the urban area's territorial expansion coincided with its growth. Coimbatore is having a lower LST range of 16.7 °C to 26.7 °C, represented in Fig. 4.

**Fig. 4: Mean LST variation in Coimbatore (a) Annual (b) Winter season and (c) Summer season**

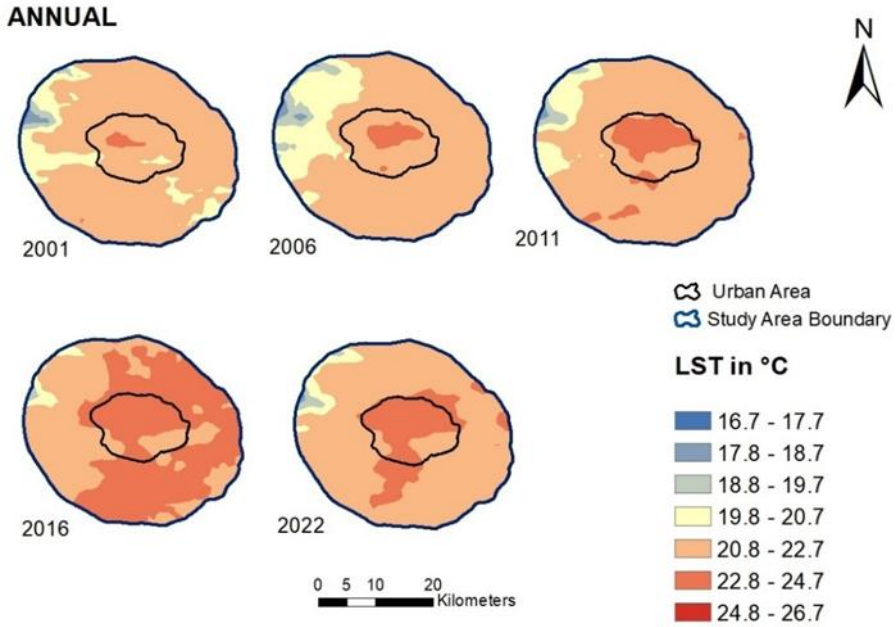


(a) Annual variation

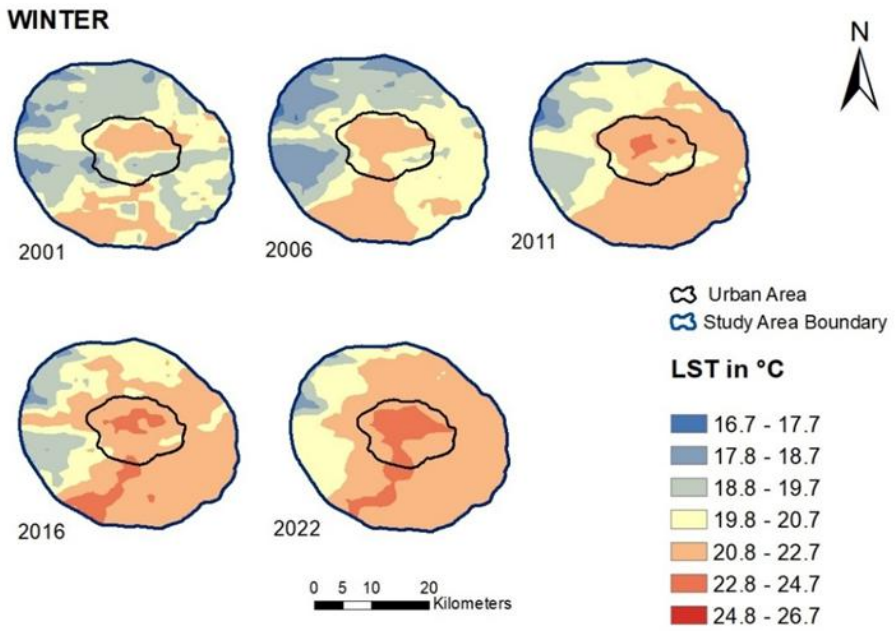


(b) Winter season

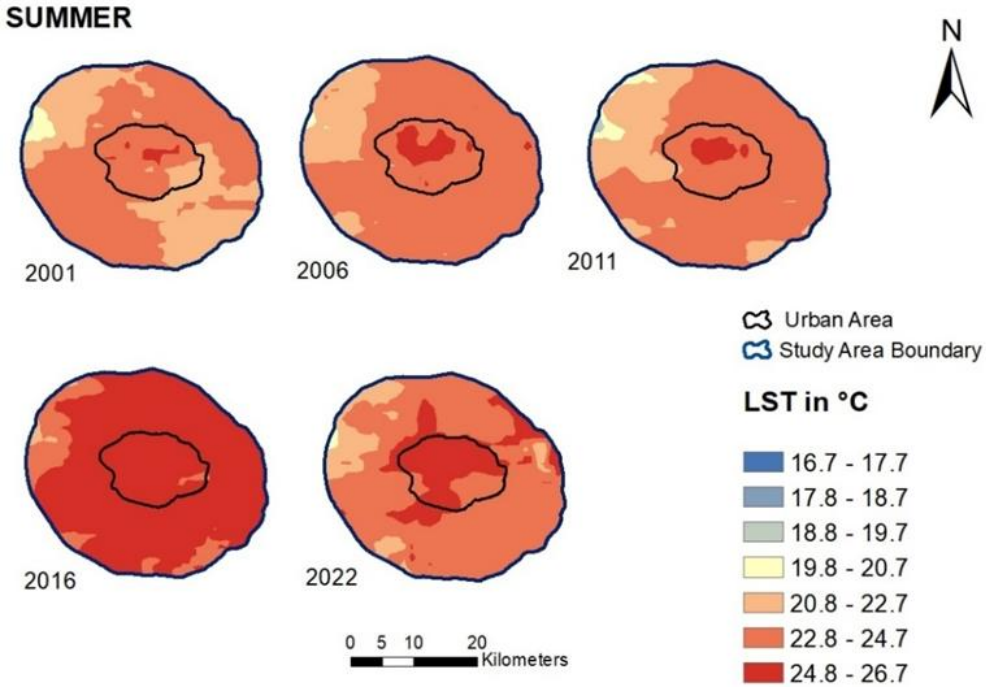


(c) Summer season

LST normally ranges between 16.7 °C and 24.7 °C during the winter season. Visual examination of the data shows a shift from 2001 to 2022 (Fig. 4 (b)). Outside of cities, blue patches denoting the lowest LSTs were seen in 2001; by 2022, these cool zones had disappeared. On the other hand, in 2022, new red patches indicating greater LSTs appeared in the south-west and close to metropolitan centres, regions that had not before seen such high temperatures.

Fig. 4(c) shows a pattern of consistently high temperatures over the summer months throughout the study area. Summer LST normally varies from 20.7 °C to 26.7 °C, with newer observations showing distinct outward geographical trends. But 2016 distinguishes out due to a discernible increase in dark red colour patches, both inside and outside of metropolitan limits, which indicate exceptionally high LSTs.

The average annual maximum, minimum, and mean LST values observed have been summarized in Table 3. The maximum annual average LST recorded for 22 years is 26.8 °C, and the minimum is 8.5 °C.

**Table 3: Variation of Mean night-time LST (°C) for the study area yearly**

| **Year** | **2001** | **2002** | **2003** | **2004** | **2005** | **2006** | **2007** | **2008** | **2009** | **2010** | **2011** |
|---|---|---|---|---|---|---|---|---|---|---|---|
| Mean | 20.6 | 21.8 | 21.4 | 21.2 | 21.4 | 20.5 | 21.3 | 21.1 | 21.4 | 22.1 | 21.2 |
| Maximum | 25.2 | 25.5 | 25.4 | 24.7 | 25.0 | 24.6 | 25.1 | 25.3 | 25.0 | 25.5 | 24.7 |
| Minimum | 8.5 | 16.7 | 16.0 | 17.3 | 15.5 | 13.9 | 15.9 | 17.8 | 13.2 | 19.2 | 16.4 |
| **Year** | **2012** | **2013** | **2014** | **2015** | **2016** | **2017** | **2018** | **2019** | **2020** | **2021** | **2022** |
| Mean | 21.8 | 22.0 | 21.3 | 21.5 | 22.4 | 22.1 | 21.4 | 22.6 | 22.2 | 21.6 | 21.4 |
| Maximum | 25.8 | 25.9 | 25.7 | 24.9 | 26.8 | 25.6 | 25.6 | 26.5 | 25.7 | 25.2 | 25.4 |
| Minimum | 18.6 | 19.3 | 10.3 | 13.2 | 19.0 | 16.9 | 16.0 | 18.5 | 18.1 | 16.9 | 10.5 |

The variation in mean night-time LST for Coimbatore from 2001 to 2022 indicates a fluctuating but discernible warming trend over the study period. During the initial decade (2001–2011), the mean night-time LST varied between 20.5 °C (recorded in 2006) and 22.1 °C (in 2010), with most years exhibiting mean values close to 21 °C, reflecting relatively stable nocturnal thermal conditions. In the subsequent decade (2012–2022), a gradual increase is observed, with mean LST values ranging from 21.3 °C (2014) to a peak of 22.6 °C (2019). The years 2016 and 2019, in particular, recorded elevated mean night-time temperatures, suggesting intensification of nocturnal warming. Although a slight decline is noted in 2021 (21.6 °C) and 2022 (21.4 °C), the overall mean LST values during the latter period remain higher than those in the early 2000s. Analysis of maximum night-time LSTs reveals a range from 24.6 °C (2006) to a maximum of 26.8 °C (2016), underscoring periods of increased thermal stress during nights. Furthermore, the minimum night-time LST displayed considerable variability, with values spanning from as low as 8.5 °C (2001) to 19.3 °C (2013). While early years experienced pronounced cold extremes during nights, the post-2010 period shows a reduction in such events, with minimum temperatures generally remaining above 16 °C, except for isolated years such as 2014 (10.3 °C) and 2022 (10.5 °C). The overall trend points toward a progressive warming of night-time LST in Coimbatore, likely driven by rapid urban expansion, modifications in land surface characteristics, and the amplification of the urban heat island effect. These findings underscore the importance of integrating sustainable urban planning strategies to mitigate future nocturnal heat stress in the region.

Also, for the study area, seasonal maximum values of LST are given in Table 4. Table 4 indicates that the year 2016 recorded the highest land surface temperature (LST) of 26.8 °C during the summer, while the winter of 2010 exhibited a temperature of 24.2 °C.

**Table 4: Maximum Mean LST (°C) for summer and winter season**

| **Max LST** | **2001** | **2002** | **2003** | **2004** | **2005** | **2006** | **2007** | **2008** | **2009** | **2010** | **2011** |
|---|---|---|---|---|---|---|---|---|---|---|---|
| Summer | 25.0 | 25.5 | 25.4 | 24.5 | 25.0 | 24.6 | 25.1 | 24.3 | 25.0 | 25.5 | 24.7 |
| Winter | 23.7 | 23.2 | 23.6 | 23.3 | 22.6 | 21.1 | 23.6 | 21.5 | 24.0 | 24.2 | 22.3 |
| **Max LST** | **2012** | **2013** | **2014** | **2015** | **2016** | **2017** | **2018** | **2019** | **2020** | **2021** | **2022** |
| Summer | 25.8 | 25.9 | 25.4 | 24.6 | 26.8 | 25.6 | 25.6 | 26.5 | 25.7 | 25.2 | 25.4 |
| Winter | 22.6 | 23.9 | 23.2 | 22.6 | 23.7 | 23.3 | 23.9 | 23.9 | 23.8 | 22.7 | 23.1 |

The analysis of maximum mean LST for Coimbatore across the summer and winter seasons from 2001 to 2022 reveals distinct seasonal thermal patterns and evolving climatic tendencies. During the summer season, the maximum mean LST exhibited relatively stable behavior between 2001 and 2011, fluctuating between 24.3 °C (2008) and 25.5 °C (2002 and 2010). However, from 2012 onward, an observable intensification in summer temperatures is evident, culminating in a peak value of 26.8 °C in 2016, followed closely by 26.5 °C in 2019. Although a marginal decrease to 25.2 °C was noted in 2021, the summer maximum mean LST consistently remained elevated compared to the early 2000s, indicative of progressively warmer summer conditions likely influenced by urbanization and anthropogenic heat emissions. In contrast, the winter season displayed comparatively modest variability in maximum mean LST. Between 2001 and 2011, winter maximums ranged from a minimum of 21.1 °C (2006) to a maximum of 24.2 °C (2010). Post-2012, winter LSTs remained relatively stable, oscillating within a narrow band between 22.6 °C and 23.9 °C, without significant extremes. The comparative analysis thus suggests that summer warming has been more pronounced than winter warming over the past two decades, underscoring the need for season-specific urban heat mitigation strategies to address the intensifying summer thermal stress in Coimbatore.

The separation of urban and rural zones facilitated the computation of mean LST over a 22-year period, as depicted in Figure 4 and outlined in Table 5. Notably, urban areas consistently exhibit higher temperatures, boasting an annual average LST of approximately 22.8 °C, with a peak of 23.7 °C. In contrast, rural areas maintain a lower average LST around 21.5 °C, reaching a maximum of 22.5 °C. Both regions display a positive trend, with urban areas (Kendall's $\tau$= 0.593) showing more than rural areas (Kendall's $\tau$= 0.429).

**Table 5: Mean LST (°C) for Urban and Rural parts yearly**

| **Year** | **2001** | **2002** | **2003** | **2004** | **2005** | **2006** | **2007** | **2008** | **2009** | **2010** | **2011** |
|---|---|---|---|---|---|---|---|---|---|---|---|
| Urban | 21.4 | 22.5 | 22.5 | 22.4 | 22.1 | 21.9 | 22.0 | 21.9 | 22.3 | 23.0 | 22.6 |
| Rural | 20.5 | 21.7 | 21.4 | 21.1 | 21.3 | 20.5 | 21.2 | 20.9 | 21.4 | 22.0 | 21.2 |
| **Year** | **2012** | **2013** | **2014** | **2015** | **2016** | **2017** | **2018** | **2019** | **2020** | **2021** | **2022** |
| Urban | 22.6 | 23.0 | 22.9 | 23.0 | 23.2 | 23.3 | 22.8 | 23.7 | 22.9 | 23.2 | 23.1 |
| Rural | 21.7 | 21.9 | 21.3 | 21.6 | 22.3 | 22.1 | 21.5 | 22.5 | 22.1 | 21.5 | 21.6 |

The analysis of mean LST for urban and rural areas of Coimbatore from 2001 to 2022 reveals a persistent and widening thermal disparity indicative of an intensifying UHI effect. Urban areas exhibited a gradual increase in mean LST from 21.4 °C in 2001 to 23.7 °C in 2019, followed by consistently elevated values above 23°C in subsequent years. In contrast, rural areas experienced a relatively moderate increase, with mean LST rising from 20.5 °C in 2001 to a peak of 22.5 °C in 2019, although subsequent years showed slight declines and greater interannual variability. The urban–rural LST differential was approximately 1 °C on average throughout the study period but exhibited a tendency to widen after 2016, particularly during periods of peak urban temperatures. The consistent elevation of urban LSTs relative to rural LSTs underscores the influence of anthropogenic factors such as increased impervious surfaces, reduced vegetation cover, and intensified human activities. The findings highlight a growing UHI effect, with implications for urban thermal comfort, energy demand, and public health, necessitating the adoption of strategic urban planning and climate-adaptive measures to mitigate future heat-related risks.

**Urban Heat Island Intensity**

The UHI intensity is defined as the LST contrast between rural and urban regions. This intensity displays both daily and seasonal variations and is influenced by meteorological elements such as clouds, wind patterns, anthropogenic heat release, and more. In this context, the average UHI intensity is determined by computing the mean LST values in urban and rural zones.

The average UHI intensity ranges annually from 0.77 °C to 1.65 °C, with an overall mean of 1.13 °C. In the winter season, the average UHII fluctuates between 0.43 °C and 1.49 °C, with an overall mean of 0.97 °C. Similarly, during the summer season, the average UHII varies from 0.5 °C to 2.22 °C, with an overall mean of 1.18 °C. UHII is found to be higher in the summer season compared to the winter season. However, the average winter UHII shows a positive trend, while the summer and annual UHII show no trend.

**Table 6: Average Annual UHI intensity (°C)**

| **Year** | **2001** | **2002** | **2003** | **2004** | **2005** | **2006** | **2007** | **2008** | **2009** | **2010** | **2011** |
|---|---|---|---|---|---|---|---|---|---|---|---|
| UHII | 0.94 | 0.83 | 1.05 | 1.22 | 0.83 | 1.44 | 0.87 | 0.96 | 0.94 | 1.08 | 1.36 |
| **Year** | **2012** | **2013** | **2014** | **2015** | **2016** | **2017** | **2018** | **2019** | **2020** | **2021** | **2022** |
| UHII | 0.81 | 1.06 | 1.64 | 1.37 | 0.94 | 1.21 | 1.26 | 1.14 | 0.77 | 1.66 | 1.46 |

**Table 7: Average Winter UHI Intensity (°C)**

| **Year** | **2001** | **2002** | **2003** | **2004** | **2005** | **2006** | **2007** | **2008** | **2009** | **2010** | **2011** |
|---|---|---|---|---|---|---|---|---|---|---|---|
| UHII | 0.61 | 0.73 | 0.43 | 0.90 | 0.61 | 1.24 | 0.89 | 1.07 | 0.98 | 0.64 | 1.20 |
| **Year** | **2012** | **2013** | **2014** | **2015** | **2016** | **2017** | **2018** | **2019** | **2020** | **2021** | **2022** |
| UHII | 0.99 | 0.74 | 1.05 | 0.92 | 0.92 | 0.92 | 1.19 | 1.49 | 1.38 | 1.27 | 1.25 |

**Table 8: Average Summer UHI Intensity (°C)**

| **Year** | **2001** | **2002** | **2003** | **2004** | **2005** | **2006** | **2007** | **2008** | **2009** | **2010** | **2011** |
|---|---|---|---|---|---|---|---|---|---|---|---|
| UHII | 0.91 | 1.03 | 0.74 | 1.40 | 1.56 | 0.92 | 0.99 | 1.33 | 0.92 | 0.66 | 1.66 |
| **Year** | **2012** | **2013** | **2014** | **2015** | **2016** | **2017** | **2018** | **2019** | **2020** | **2021** | **2022** |
| UHII | 1.02 | 2.22 | 1.00 | 2.12 | 1.73 | 0.89 | 1.23 | 0.71 | 0.64 | 0.50 | 1.89 |

**Average Annual UHI Intensity**

Table 6 displays the average annual UHI intensity of the Coimbatore study area. The analysis of average annual Urban Heat Island Intensity (UHII) for Coimbatore from 2001 to 2022 indicates notable interannual variability with a subtle long-term upward trend. During the initial period (2001–2011), the annual UHII values fluctuated between 0.83 °C (2002 and 2005) and 1.44 °C (2006), with an average intensity typically around 1.0 °C. The year 2006 exhibited the highest annual UHII (1.44 °C) within this period, highlighting a significant urban-rural thermal contrast. Moving into the later period (2012–2022), UHII values became more variable, reaching a minimum of 0.77°C (2020) and a maximum of 1.66 °C (2021). Particularly, 2014 (1.64 °C) and 2021 (1.66 °C) recorded markedly high annual UHI intensities, suggesting periods of amplified urban warming relative to rural areas. Overall, the data reveal that while annual UHI intensity fluctuates, there is evidence of a general strengthening of the UHI phenomenon over time, possibly driven by continued urban expansion, increased impervious surfaces, and reduced vegetation cover in Coimbatore.

**Average Winter UHI Intensity**

Table 7 represents the average winter UHI intensity of the Coimbatore study area. The examination of average winter UHII from 2001 to 2022 shows a pattern of progressive intensification with some interannual variability. In the early phase (2001–2011), winter UHII values ranged from 0.43 °C (2003) to 1.24 °C (2006), with notable peaks in 2006 and 2011 (1.20 °C). The relatively low winter UHII values in years like 2003 (0.43 °C) and 2005 (0.61 °C) suggest that earlier winters experienced less pronounced urban-rural thermal contrasts. However, from 2012 onwards, a consistent increase is observed, with winter UHII exceeding 1.0 °C in most years. Noteworthy are the years 2019 (1.49 °C) and 2020 (1.38 °C), which exhibited the highest winter UHI intensities in the study period, indicative of a significant warming of urban areas even during the cooler season. This intensification of winter UHII over time suggests that Coimbatore's urbanization effects persist year-round, reducing seasonal thermal relief traditionally associated with winter months.

**Average Summer UHI Intensity**

Table 8 shows the average summer UHI intensity of the Coimbatore study area. The evaluation of average summer UHII from 2001 to 2022 reveals greater variability compared to winter and annual patterns, reflecting complex interactions between seasonal heating, land cover, and urban morphology. Between 2001 and 2011, summer UHII values varied from a low of 0.66 °C (2010) to a peak of 1.66 °C (2011), with multiple years, such as 2005 (1.56 °C) and 2004 (1.40 °C), showing intensified summer UHI effects. The post-2012 period is marked by significant fluctuations, with extremely high summer UHII recorded in 2013 (2.22 °C) and 2015 (2.12 °C), indicating severe urban heat amplification during these years. However, a noticeable decline in summer UHII is observed after 2016, with values dropping to as low as 0.50 °C in 2021 before rebounding to 1.89 °C in 2022. These variations suggest that while certain years experienced extreme summer UHI conditions, the overall trend post-2016 has been more erratic, possibly influenced by episodic climatic variations, localized urban planning interventions, or transient environmental factors.

**Trend Analysis**

A key observation is that the positive S values across all graphs suggest a general trend of increasing value over time. The average UHI and LST displayed a positive Sen's slope (beta) value. In the context of Sen's slope (b), greater than 0 signifies an upward trend in the time

series, while a b less than 0 would indicate a downward trend. The significance of the trends was assessed using the p-value, with a significance level of 0.05. A p-value less than 0.05 indicates a monotonic trend.

A notable and statistically significant trend is identified for urban LST with a Kendall's tau value of 0.593 and a Sen's slope of 0.072. This finding is consistent with the trend, further supporting the observed upward trend in urban LST over the analyzed period. Similar to urban LST, rural LST also shows a discernible trend, albeit to a lesser extent. This evidence shows that LST trends can be seen in both cities and the countryside. In the winter season, the average UHII is found to have a positive trend, as indicated by a Kendall's tau of 0.506 and a Sen's slope of 0.03. This finding indicates a rising trend in UHII throughout winter. However, for average summer and annual UHII, no significant trend is detected, implying variability without a clear monotonic trend over time during the study period of 22 years. The trend analysis result is shown in Table 9.

**Table 9: Mann-Kendall Test Analysis for Coimbatore**

| Variable | Kendall's τ | S | Var (S) | P Value | Alpha | Sen's Slope | Sen's intercept | Significant Trend |
|---|---|---|---|---|---|---|---|---|
| Annual UHII | 0.29 | 67 | 1257 | 0.063 | 0.05 | 0.019 | 0.885 | No |
| Winter UHII | 0.506 | 117 | 1257 | 0.001 | 0.05 | 0.03 | 0.632 | Yes |
| Summer UHII | -0.022 | -5 | 1257 | 0.91 | 0.05 | -0.002 | 1.025 | No |
| Urban LST | 0.593 | 137 | 1257 | 0.0001 | 0.05 | 0.072 | 21.78 | Yes |
| Rural LST | 0.429 | 99 | 1257 | 0.006 | 0.05 | 0.048 | 20.94 | Yes |

The Mann-Kendall trend analysis for Coimbatore, as presented in Table 9, provides a comprehensive statistical evaluation of the temporal trends in UHII and LST for both urban and rural areas. The results for annual UHII reveal a Kendall's τ value of 0.29 with a p-value of 0.063, indicating a positive but statistically non-significant trend at the 5 % significance level. The Sen's slope estimates of 0.019 further suggests a slight upward tendency in annual UHII, although the trend cannot be considered robust. In contrast, winter UHII exhibits a statistically significant increasing trend, with a Kendall's τ of 0.506, a p-value of 0.001, and a Sen's slope of 0.03, signifying a steady intensification of winter-time urban heat island effects over the study period. Meanwhile, summer UHII shows a Kendall's τ of -0.022 and a p-value of 0.91, indicating no significant trend and suggesting substantial variability or stabilization in summer UHI behavior.

For LST, both urban and rural areas display statistically significant increasing trends. Urban LST shows a strong positive trend with a Kendall's τ of 0.593 and a highly significant p-value of 0.0001, accompanied by a Sen's slope of 0.072, reflecting a notable rate of temperature increase over time. Similarly, rural LST also demonstrates a significant positive trend, with a Kendall's τ of 0.429 and a p-value of 0.006, although the rate of increase (Sen's slope = 0.048) is slightly lower than that of urban areas. These findings clearly illustrate that while both urban and rural regions are experiencing warming, the magnitude and consistency of warming are more pronounced within urban environments. Overall, the results highlight

the critical issue of accelerating urban thermal stress, particularly during winter months, and underscore the urgent need for climate-responsive urban planning strategies in Coimbatore.

**$UHI_{index}$**

The $UHI_{index}$ represents the normalized LST of all pixels in the study area. For the 22-year study period, 1056 night-time LST images are available. Images are obtained for the annual, winter, and summer seasons by using the mean data at an interval of 5 years from 2001 to 2022. The $UHI_{index}$ variations are shown below for the Coimbatore study area.

This study revealed interesting spatial and temporal variations in the $UHI_{index}$ for Coimbatore, contrasting with observations. UHI intensity typically exhibits a well-defined spatial pattern; Coimbatore's $UHI_{index}$ displayed a more random distribution across the study area. This lack of a clear spatial trend was observed throughout the year but became particularly pronounced during the winter season.

Despite the absence of a strong spatial pattern, a concerning trend emerged when analyzing the $UHI_{index}$ across seasons. While both winter and summer exhibited a weak positive trend in UHI intensity, with the highest values (0.9 to 1) consistently occurring within the urban core, a more significant increase was evident when examining annual data. This annual rise suggests a long-term intensification of the UHI effect in Coimbatore. The observed discrepancy between Coimbatore and other cities likely stems from variations in the built environment. Furthermore, the specific distribution of built-up areas within Coimbatore may contribute to the observed randomness in UHI intensity.

**Fig. 5: $UHI_{index}$ variation in Coimbatore (a) Annual variation, (b) Winter season (c) Summer season**

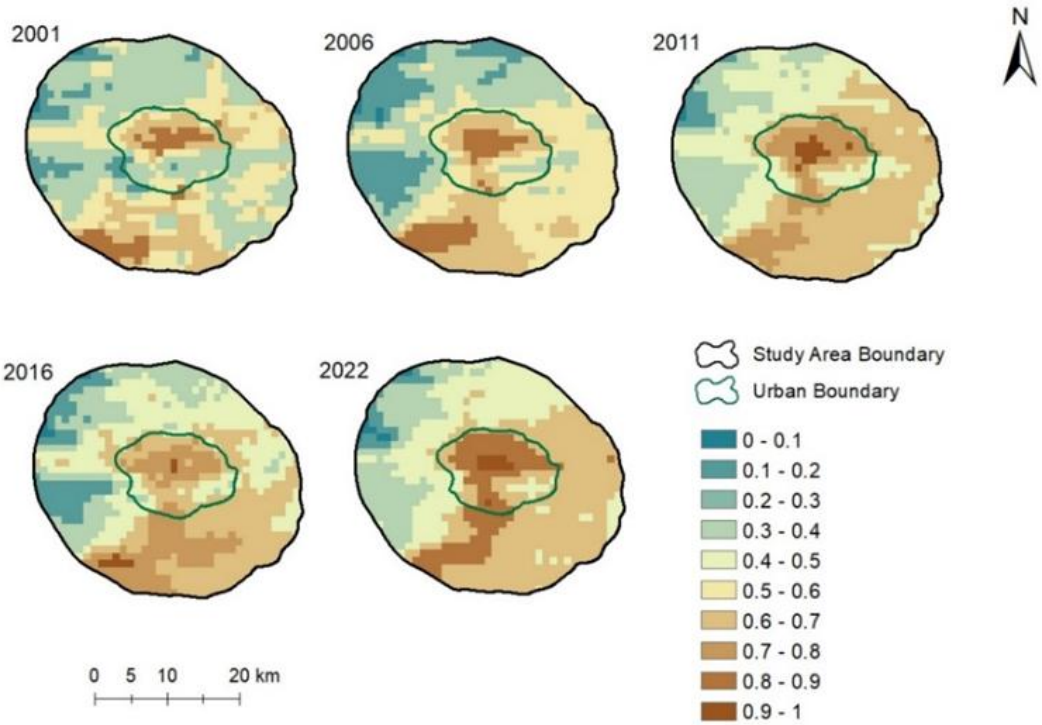

(a) Annual variation

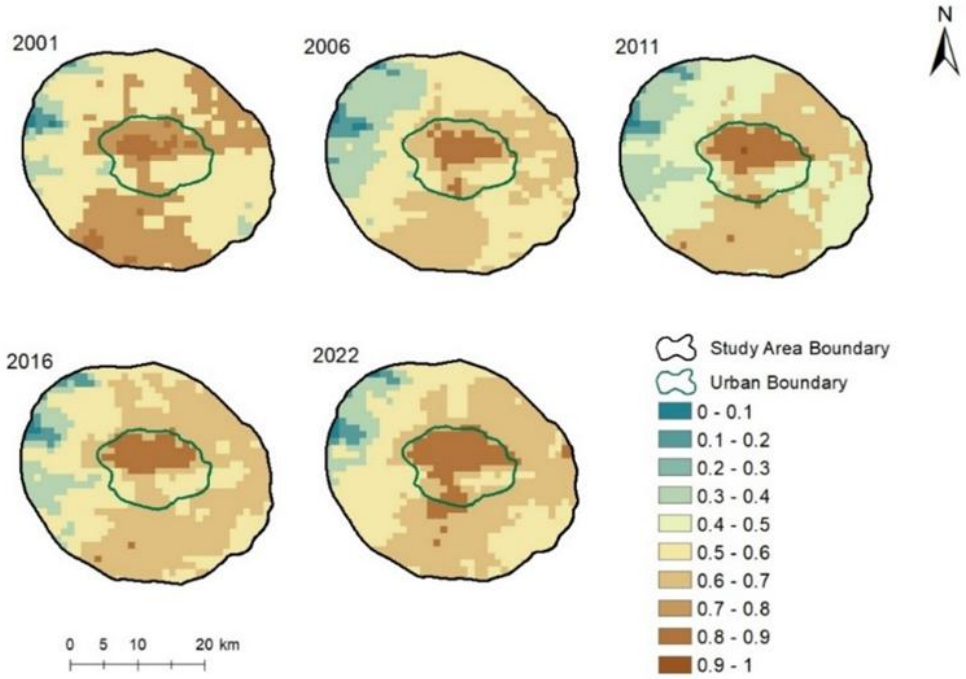


(b) Winter season

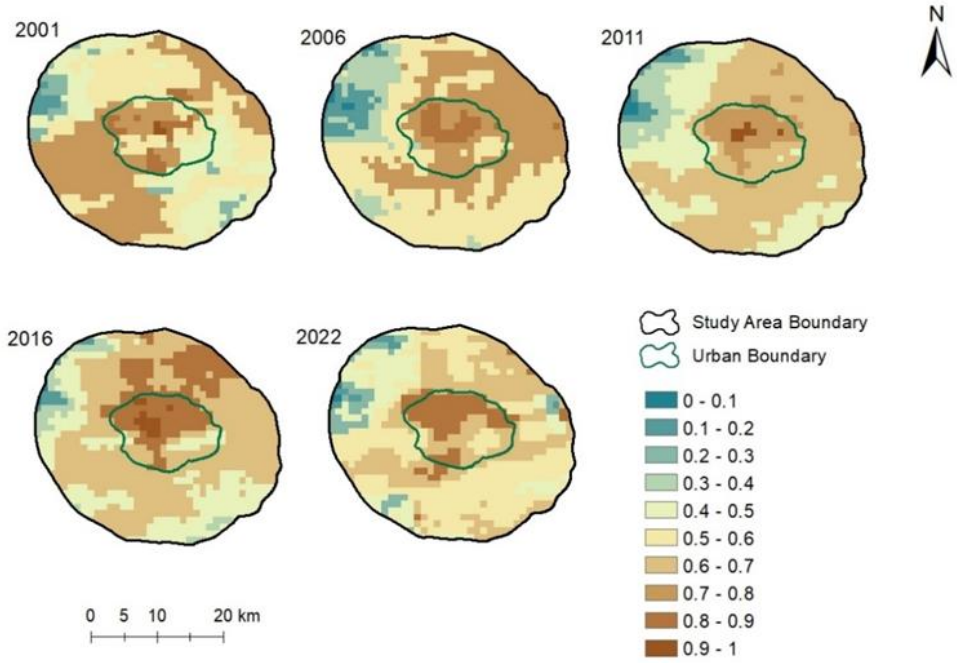


(c) Summer season

Fig. 5 shows the $UHI_{index}$ variation in Coimbatore across three temporal scales: annually, during winter, and during summer. Although exact numerical values are not specified in the figure, a qualitative and comparative analysis can be made based on the visible patterns.

Annually, the $UHI_{index}$ displays moderate fluctuations, indicating the persistence of heat accumulation throughout the year, with peak intensities likely occurring during pre-monsoon and summer months. This consistent urban–rural thermal contrast points to continuous anthropogenic heat emissions and land surface changes due to urbanization.

During the winter season, the $UHI_{index}$ tends to be relatively lower compared to summer, with smaller amplitude variations. This can be attributed to reduced solar radiation and generally lower atmospheric temperatures, resulting in a less pronounced heat retention in urban areas. However, some elevated UHI instances may still be observed, possibly due to nighttime heat retention and lower wind speeds during this period.

In contrast, the summer season exhibits the highest $UHI_{index}$ values. The elevated temperatures, coupled with increased anthropogenic activities and higher impervious surface heat retention, amplify the urban–rural temperature differential. The spatial extent and intensity of UHI are more prominent in this season, reflecting the compounded effect of climatic and urban factors.

Overall, the analysis confirms that the UHI effect in Coimbatore is seasonally dependent, with summer showing the most intense UHI manifestations. This seasonal trend underlines the need for targeted urban climate mitigation strategies, especially during warmer periods.

**Thermal Hotspot Analysis**

A hotspot is a collection of pixels with higher temperatures. However, only a large proportion of those pixels are considered hotspot areas or zones, which have statistical importance. The Hotspot Spatial Auto-correlation Analysis (Moran's index) is used to determine the hotspot creation pattern and significance, and the results are shown in this section for summer and winter, as well as 22-year mean $UHI_{index}$ images. The fixed distance method is used to conceptualize spatial relationships, and the distance and Euclid's approach are the current distance methods.

Fig. 6 represents the thermal classification of Coimbatore (2001-2022), winter and summer seasons. All the hot spots with 99 % confidence levels (CL) are within the urban boundary; these are the areas with the highest LST in the entire study area. The average temperature in this zone is in the range of 24.8 °C to 26.7 °C. The hot spots with 99 % CL have expanded spatially in the urban core, with an increase in the LST over time. On the other hand, the spatial extent of hotspots with 95 % and 90 % CL has remained almost the same, although LST has risen over time. During the analysis, cold spots of 99 % confidence level were identified in Coimbatore. However, no substantial increase or decrease of cold patches in Coimbatore is observed. High risk zones are depicted in Fig. 6 (a).

**Fig. 6: Thermal classification of Coimbatore (a) Annually (2001-2022), (b) Winter season and (c) Summer season**

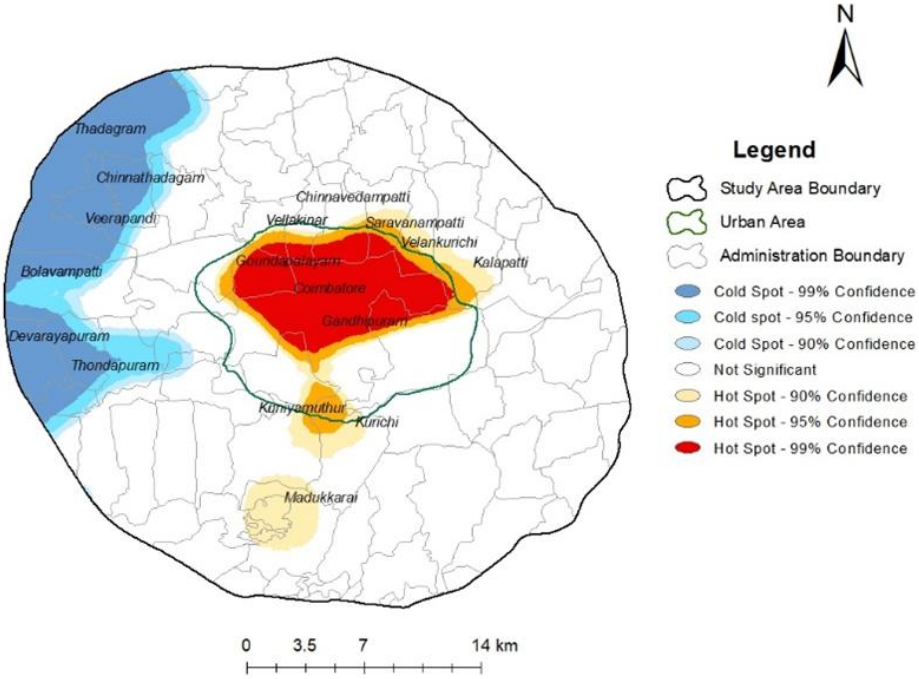


a) Annual

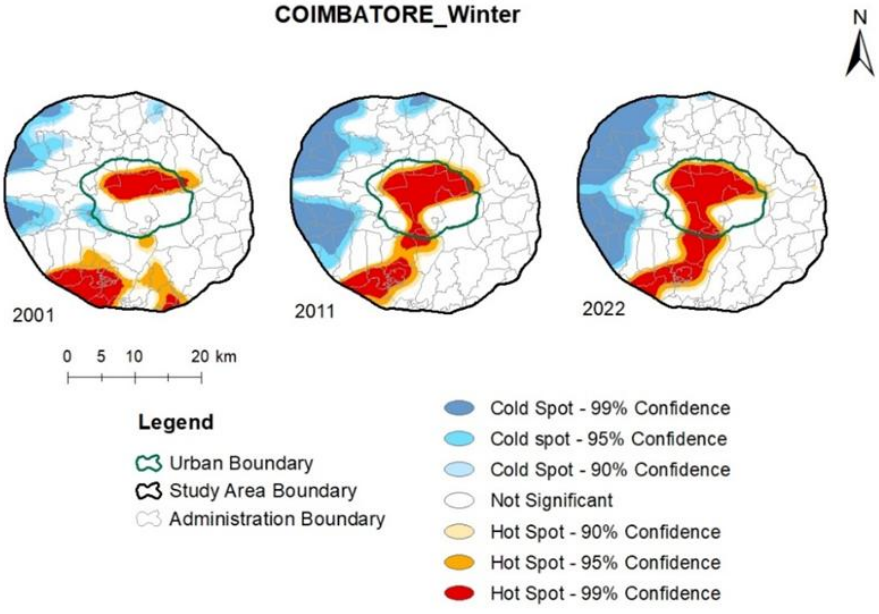


(b) Winter season

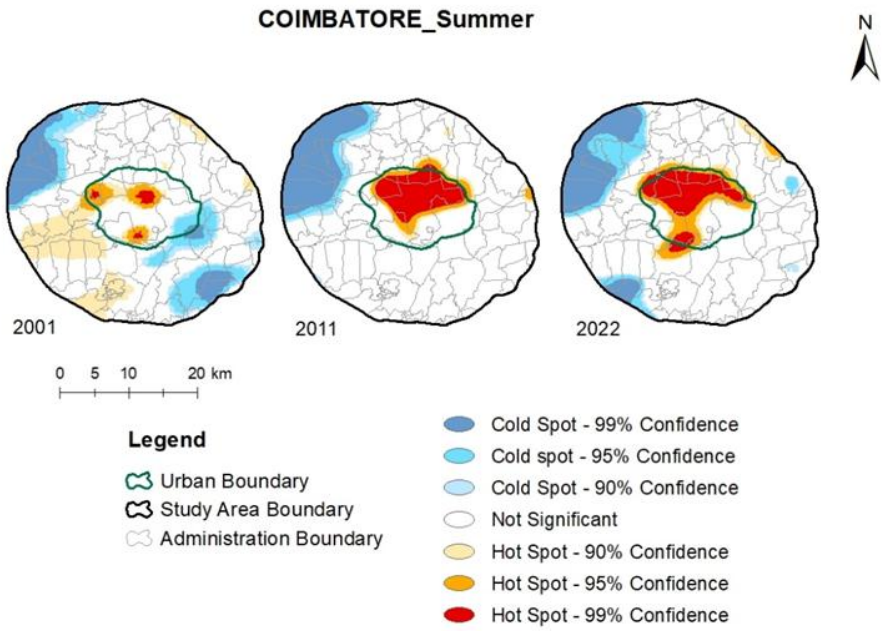


(c) Summer season

In Table 10, z-scores for 2001, 2011, and 2022 (42.25, 44.809, and 45.445, respectively) show that the clustered pattern of hot or cold regions is unlikely to be caused by coincidence. The Global Moran's I statistic shows that hot and cold locations are statistically significant. The z-score of the thermal classification of Coimbatore for the 22-year average LST is 45.424 (Table 10). Over the previous 22 years, the average LST outside the Coimbatore urban boundary has been 16.7 °C to 22.7 °C.

**Table 10: Spatial correlation analysis result for mean LST Annually**

| Year | 2001 | 2011 | 2022 | 22 years |
|---|---|---|---|---|
| **Moran's Index** | 0.797 | 0.845 | 0.857 | 0.857 |
| **Variance** | 0.0003 | 0.0003 | 0.0003 | 0.0003 |
| **z-score** | 42.253 | 44.809 | 45.445 | 45.424 |
| **p-value** | 0.000 | 0.000 | 0.000 | 0.000 |

Hot and cold spots have been identified for both the winter and summer seasons. Tables 11 and 12 provide the z-scores for Coimbatore's thermal categorization for winter and summer LST, respectively. Fig. 6 (b and c) depicts the spatial and temporal change of thermal zones within the research region throughout the winter and summer, respectively. Cold areas with 99 % CL are observable in the winter and summer, but only outside the urban limit and mostly near the rural boundary.

An analysis of hot spots, defined as areas with exceptionally high LST, revealed a concerning trend of spatial expansion across both winter and summer seasons, particularly during the summer months. Interestingly, winter exhibited a unique characteristic where some hot spots were identified outside the urban boundary. This may be attributed to the clustering of pixels with high LST values. Several specific areas, including Goundapalayam, Ghandhipuram, Kalapatti, Vellakinar, and Velankuruchi, were consistently identified as hot spots with a 99 % confidence level.

The annual thermal classification of Coimbatore **from 2001 to 2022** reveals a noticeable shift toward higher thermal zones over time. A significant increase in **very high thermal zones** is evident, suggesting intensified surface heating in urban areas. This progression is strongly linked to rapid urban expansion, reduced vegetation cover, and increased impervious surfaces that trap more heat. The persistent rise in high thermal zones underscores the growing UHI effect in Coimbatore, emphasizing the urgent need for climate-sensitive urban planning and green infrastructure to mitigate heat stress and promote thermal comfort.

**Table 11: Spatial correlation analysis result for mean LST for winter season**

| Year | 2001 | 2011 | 2022 |
|---|---|---|---|
| **Moran's Index** | 0.812 | 0.873 | 0.903 |
| **Variance** | 0.000 | 0.000 | 0.000 |
| **z-score** | 42.998 | 46.244 | 47.848 |
| **p-value** | 0.000 | 0.000 | 0.000 |

**Table 12: Spatial correlation analysis result for mean LST for summer season**

| Year | 2001 | 2011 | 2022 |
|---|---|---|---|
| **Moran's Index** | 0.801 | 0.869 | 0.832 |
| **Variance** | 0.000 | 0.000 | 0.000 |
| **z-score** | 42.458 | 46.103 | 44.088 |
| **p-value** | 0.000 | 0.000 | 0.000 |

While the temperature range in Coimbatore is generally lower, potentially offering some thermal comfort to residents in these hot spot zones, the elevated LSTs could still lead to increased energy demands for cooling purposes. This highlights the potential impact of UHIs even in cities with relatively moderate temperatures.

The spatial correlation hotspot analysis of mean LST in Coimbatore for annual, winter, and summer seasons over selected years (2001, 2011, and 2022) reveals a strong and consistent clustering pattern of high-temperature zones across the city.

Annually, Moran's Index increased from 0.797 in 2001 to 0.857 in 2022, indicating an intensification in the spatial clustering of high LST values over the two decades. The consistently high z-scores (rising from 42.253 to 45.445) and p-values of 0.000 confirm statistically significant clustering, pointing to a growing concentration of heat-prone areas due to urban expansion and reduced vegetation.

In the winter season, Moran's Index rose more steeply from 0.812 (2001) to 0.903 (2022), with corresponding z-scores increasing from 42.998 to 47.848. This suggests that even in cooler months, the spatial clustering of warmer areas has intensified, likely due to persistent

heat retention in built-up surfaces and the reduction of cooling effects from natural land covers.

During the summer season, the index grew from 0.801 in 2001 to 0.869 in 2011, followed by a slight decrease to 0.832 in 2022. Despite this minor dip, the values still indicate strong spatial autocorrelation. The peak z-score of 46.103 in 2011, followed by 44.088 in 2022, continues to affirm significant clustering of hot zones, although the slight decline may reflect spatial redistribution of hotspots or microclimatic interventions in some areas.

Overall, the results clearly indicate a persistent and statistically significant spatial clustering of high LST zones across all seasons, driven by increasing urbanization, land use changes, and anthropogenic heat emissions. These findings underscore the critical need for spatially targeted mitigation strategies, such as green infrastructure and urban cooling interventions, especially in hotspot zones.

## DISCUSSION

The long-term analysis of nighttime LST and UHII in Coimbatore from 2001 to 2022 reveals an intensifying urban thermal environment, in line with global urbanization trends. The increase in urban nighttime LST from 21.4 °C to 23.7 °C and the widening urban–rural differential, particularly after 2016, suggest a growing UHI effect, consistent with findings from other Indian cities such as Delhi, Bangalore, Mumbai, and Hyderabad (Arunab & Mathew, 2024; Kikon *et al*., 2016; Chakraborty & Lee, 2019). Case studies in rapidly urbanizing Indian cities such as Ahmedabad, Jaipur, Chandigarh, and Bengaluru likewise report significant links between land-cover change and rising nighttime LST, reinforcing that urbanization-driven surface modification is a dominant factor in nocturnal warming (Khandelwal *et al*., 2018; Mathew *et al*., 2024; Mohammad & Goswami, 2021). The observed long-term increase in nighttime LST and the intensification of urban thermal clustering in Coimbatore are consistent with recent findings from both regional and international studies. Several Indian studies report persistent nighttime warming and stronger urban than rural LST trends, linked to urban expansion and land-cover change (Mathew *et al*., 2018; Gupta *et al*., 2020). Our results—showing an urban LST rise exceeding that of rural areas and pronounced clustering of high-temperature zones—align with these regional patterns and confirm that mid-sized cities are experiencing UHI intensification similar to larger metropolitan areas. Recent reviews also note an increasing focus on UHI impacts in South Asia and reinforce the role of urbanization and loss of vegetation in driving surface warming (Cheval *et al*., 2024). The observed rise in nighttime LST across Coimbatore between 2001 and 2022 can be attributed to a complex interplay of anthropogenic and biophysical factors associated with rapid urbanization. One of the primary drivers is the expansion of impervious surfaces, including concrete pavements, rooftops, and built-up structures, which exhibit high heat storage capacity during the day and gradually release stored energy after sunset (Zhou *et al*., 2015; Mathew *et al*., 2018). This process significantly reduces nocturnal cooling efficiency, resulting in a sustained elevation of nighttime surface temperatures. The thermal inertia of urban materials such as asphalt and concrete prolongs heat retention, thereby intensifying the nighttime UHI effect (Mathew *et al*., 2018; Wang *et al*., 2025b).

The spatial autocorrelation analysis using Moran's I and z-scores provides robust evidence of statistically significant clustering of high-temperature zones. The annual Moran's Index rising from 0.797 to 0.857 and winter values peaking at 0.903 by 2022 highlight persistent and growing spatial patterns of heat concentration. Similar patterns were observed in studies

conducted in Ahmedabad and Chennai (Sahana *et al*., 2018; Mathew *et al*., 2022), affirming the role of impervious surface expansion and vegetation loss in intensifying urban thermal loads. The consistent expansion of hotspots with 99 % confidence levels within the urban core (with temperatures ranging from 24.8 °C to 26.7 °C) aligns with evidence from satellite-derived thermal classifications in tropical cities (Zhao *et al*., 2014; Weng *et al*., 2004). These spatial changes emphasize the thermal vulnerability of densely built environments and the necessity for spatially explicit climate adaptation strategies. Gupta *et al*. (2020) documented changes in surface heat patterns associated with land-use shifts and reductions in evapotranspiration—mechanisms we also identify for Coimbatore, where impervious surface growth and vegetation decline correspond with hotspot expansion. Similarly, a municipality-level analysis of Coimbatore and nearby districts indicates increasing LST trends and localized decreases in cold extremes. Vegetation loss also plays a critical role in nighttime warming. The reduction in vegetative cover limits evapotranspiration and decreases surface moisture availability, which otherwise facilitates latent heat fluxes and promotes cooling (Neha *et al*., 2020). In the context of Coimbatore, the conversion of peri-urban agricultural and vegetated areas into residential and industrial zones has diminished the natural capacity for nocturnal heat dissipation. Furthermore, reduced vegetation contributes to lower surface emissivity heterogeneity, leading to more uniform and persistent nighttime heat accumulation. Another significant factor is the emission of anthropogenic heat from transportation, domestic energy consumption, and industrial activities. Heat generated from vehicles, air conditioning units, and manufacturing processes accumulates in the urban canopy, especially during late evening hours when the atmospheric mixing layer is shallow (Wu *et al*., 2024). This trapped heat further elevates nighttime LST values, exacerbating the disparity between urban and rural thermal conditions.

Additionally, UHII trends show seasonal variability, with summer intensification being particularly concerning. The interannual variability and the peak LST of 26.8 °C in 2016 mirror extreme heat trends reported in other semi-arid Indian urban centers (Jain *et al*., 2020). Zhang *et al*. (2025) found that regional surface urban heat island intensity (RSUHII) in the Beijing–Tianjin–Hebei urban agglomeration increased 2.7-fold from 2005 to 2020, evolving from scattered to large-scale heat zones. They observed that socioeconomic factors, especially industrial density, became the main drivers of RSUHII, surpassing natural factors. The study highlights that urbanization and industrial redistribution strongly shape regional thermal environments, emphasizing the need for climate-resilient urban planning. The statistically significant Mann–Kendall trend results for winter UHII and urban LST further corroborate the long-term warming trend. The stronger winter clustering and year-round persistence of elevated LST clusters in Coimbatore mirror findings in other Indian cities where nighttime SUHI intensification is often more evident during calmer, drier seasons when radiative cooling is limited (Mohammad & Goswami, 2021; Badugu *et al*., 2023). Seasonal variability in SUHI (peaks in some summers, intensification in winters) likely reflects the interplay of monsoonal moisture, cloud cover, and seasonal vegetation dynamics that modulate surface energy exchanges. Moreover, Coimbatore's local topography (proximity to the Western Ghats and basin-like features) may reduce nocturnal ventilation in some urban cores, exacerbating heat trapping—an effect observed in other topographically influenced urban areas. Atmospheric conditions—particularly reduced wind speed, cloud cover, and temperature inversions—further reinforce nighttime UHI intensity (Ngarambe *et al*., 2021). These meteorological factors limit radiative and convective cooling, promoting heat retention within the lower boundary layer. In tropical and subtropical climates such as Coimbatore, where calm and humid nights are frequent, the combined influence of anthropogenic heat and limited radiative loss contributes to pronounced nighttime warming.

Topographical influences also modulate nighttime LST variations. Coimbatore's semi-basin morphology, surrounded by the Western Ghats, may hinder nocturnal ventilation and facilitate heat trapping in low-lying urban cores. This geographical setting amplifies the persistence of elevated nighttime temperatures compared to open rural surroundings. The combined evidence indicates that three interlinked factors primarily explain the rise in nighttime LST in Coimbatore: (1) expansion of impervious surfaces and built-up density, which increases heat storage and delays nocturnal cooling; (2) vegetation loss and reduced evapotranspiration, which diminish latent cooling fluxes; and (3) anthropogenic heat emissions from transport, industry, and domestic energy use that raise the nocturnal energy budget. These mechanisms are supported by recent empirical and modelling studies in India and elsewhere that highlight thermal inertia of urban materials, reduced evapotranspiration, and trapped anthropogenic heat as dominant drivers of nighttime UHI intensification.

These findings strongly advocate for urban climate-responsive planning interventions. Strategies such as enhancing green infrastructure, promoting high-albedo materials, and regulating land use intensification are critical to mitigate UHI effects (Santamouris, 2015; Li *et al*., 2017). Given the projected rise in urban population and temperature extremes due to climate change, cities like Coimbatore must prioritize resilient urban design to protect public health and improve livability. The intensification of nighttime LST reflects the synergistic effects of land cover transformation, anthropogenic heat emissions, and atmospheric stability. Similar trends have been observed in other Indian cities such as Bengaluru and Hyderabad (Arunab & Mathew, 2023), reinforcing the regional consistency of urban-induced nighttime warming across peninsular India. These findings emphasize the urgency of integrating climate-sensitive urban design, including enhanced green infrastructure, reflective roofing materials, and improved ventilation corridors, to counteract heat storage and facilitate nocturnal cooling. Our spatially explicit identification of persistent hotspots offers immediate guidance for urban practitioners. Municipal authorities and planners should prioritize interventions in mapped high-confidence hotspots (99 % CL), including: (i) increasing urban green cover (street trees, pocket parks, and green roofs) targeted to hotspot neighborhoods; (ii) deploying high-albedo/reflective materials on roofs and pavements to reduce heat storage; (iii) preserving and restoring peri-urban vegetation to strengthen nocturnal cooling and evapotranspiration; and (iv) integrating UHI risk maps into zoning, building codes, and Heat Action Plans. Evidence from recent policy-oriented studies indicates that such measures reduce surface and near-surface temperatures and also yield co-benefits for air quality and public health, particularly for vulnerable groups. Implementing these measures in mid-sized cities like Coimbatore can be both cost-effective and rapidly actionable.

## CONCLUSIONS

The long-term assessment of nighttime LST in Coimbatore from 2001 to 2022 reveals a progressive warming trend, with urban areas experiencing a mean LST increase from 21.4 °C in 2001 to 23.7 °C in 2019, while rural areas showed a more moderate rise from 20.5 °C to 22.5°C during the same period. The average annual urban–rural LST differential remained around 1°C but widened significantly after 2016, coinciding with a peak summer LST of 26.8 °C. The highest annual maximum nighttime LST recorded was also 26.8 °C in 2016, while the lowest minimum was 8.5 °C in 2001, indicating a decline in cold extremes over time. Seasonal analysis showed that summer LSTs have intensified more than winter LSTs, with maximum mean summer LST increasing from 24.3 °C (2008) to 26.8 °C (2016),

whereas winter values remained relatively stable between 22.6 °C and 24.2 °C post-2012. Kendall's tau values further confirm this warming trend, with urban areas ($\tau$ = 0.593) showing a stronger positive correlation than rural zones ($\tau$ = 0.429). The analysis of average UHII across annual, winter, and summer periods from 2001 to 2022 in Coimbatore reveals a consistent yet seasonally variable intensification of the UHI phenomenon. Annual UHII trends indicate a gradual strengthening of urban-rural thermal contrasts over time, with notable peaks in 2014 and 2021, reflecting the cumulative impacts of urbanization and land surface modification. Winter UHII patterns demonstrate a progressive rise, particularly after 2012, suggesting a diminishing seasonal cooling effect in urban areas and highlighting the year-round persistence of elevated urban temperatures. In contrast, summer UHII trends exhibit greater interannual variability, with extreme intensifications observed in 2013 and 2015, followed by a temporary decline post-2016 and a resurgence in 2022. Collectively, these findings underscore the dynamic and evolving nature of UHI intensity in Coimbatore, driven by a combination of urban growth, changing land use patterns, and climatic variability. They highlight the urgent need for climate-adaptive urban strategies—such as greening, sustainable design, and thermal comfort planning—to mitigate rising UHI impacts on health, energy use, and livability. The Mann-Kendall test results indicate a statistically significant increasing trend in winter UHII, urban LST, and rural LST, while annual UHII and summer UHII show no significant trends. The urban LST exhibits the highest rate of increase, highlighting intensified urban warming relative to rural areas. The $UHI_{index}$ in Coimbatore exhibits clear seasonal variation, with the highest intensity during summer and the lowest during winter. This pattern highlights the influence of climatic conditions and urban infrastructure on heat accumulation, underscoring the need for targeted mitigation strategies, especially in the summer months, to enhance urban thermal comfort and resilience.

The spatial correlation analysis confirms that Coimbatore has experienced a significant and growing clustering of high LST zones from 2001 to 2022 across annual, winter, and summer seasons. The increasing Moran's Index and z-scores reflect the intensifying UHI effect, with heat-prone areas becoming more spatially concentrated over time. This pattern is especially prominent during the winter and annual periods, indicating year-round thermal stress. The hotspot spatial autocorrelation analysis for Coimbatore over the 22-year period (2001–2022) reveals a statistically significant intensification in the clustering of high-temperature zones, with Moran's Index rising from 0.797 to 0.857 annually and corresponding z-scores increasing from 42.253 to 45.445, indicating non-random, persistent thermal clustering. In the winter season, Moran's Index showed the steepest increase—from 0.812 in 2001 to 0.903 in 2022—accompanied by z-scores escalating from 42.998 to 47.848, signifying heightened cold-season urban heating. Summer showed a peak Moran's Index of 0.869 in 2011 before a marginal drop to 0.832 in 2022, with z-scores remaining high (46.103 in 2011 and 44.088 in 2022), confirming strong spatial autocorrelation. Hotspots with a 99 % confidence level (CL) were confined within the urban core and expanded over time, with average temperatures in these zones ranging from 24.8 °C to 26.7 °C. Meanwhile, cold spots with 99 % CL remained predominantly in rural areas without significant expansion or contraction.

The present study makes several key contributions. First, it provides a comprehensive spatio-temporal assessment of nighttime LST and UHI intensity in Coimbatore over a 22-year period, revealing statistically significant warming trends and seasonal variations. Second, it demonstrates the spatial clustering and intensification of urban heat zones using Moran's Index and hotspot analysis, offering a robust methodological framework for UHI studies. Third, the study links urbanization and impervious surface growth to UHI intensification, providing actionable insights for urban planning and climate adaptation

strategies. Finally, by integrating spatial analysis with policy-relevant recommendations, the study offers practical guidance for municipal authorities, urban planners, and community organizations to mitigate heat stress and enhance urban livability. The long-term assessment of nighttime LST in Coimbatore from 2001 to 2022 demonstrates a persistent warming trend, with urban areas exhibiting a stronger increase compared to rural zones. The intensification of the UHI effect, particularly in winter and in high-density urban clusters, underscores the impact of urban expansion, declining vegetation, and increasing impervious surfaces. These findings have clear implications for urban planning and policy. Strategies such as expanding green cover, implementing reflective or high-albedo surfaces, and adopting climate-sensitive urban design can reduce urban thermal stress and enhance resilience. Municipal authorities and urban planners can utilize the spatial UHI maps and hotspot analyses to prioritize high-risk neighborhoods for intervention, while community organizations can engage in local greening and awareness initiatives to mitigate heat exposure. By translating these insights into actionable measures, the study provides a framework for evidence-based decision-making to address UHI effects and improve urban livability.

**Limitations**

Despite the robustness of satellite-derived LST data in capturing spatial and temporal thermal patterns, certain limitations and uncertainties should be acknowledged. The spatial resolution of MODIS data may not fully represent the fine-scale heterogeneity of urban microclimates, especially in densely built environments. Additionally, emissivity assumptions used in the retrieval algorithm can introduce bias, particularly across heterogeneous surfaces comprising vegetation, water, and impervious materials. Atmospheric effects, including variations in water vapor and aerosol content, may further influence LST accuracy despite standard atmospheric corrections. These inherent uncertainties emphasize the importance of in-situ validations and the integration of high-resolution or multi-sensor datasets in future studies to refine urban thermal assessments.

**Future Scope**

Future studies could focus on assessing canopy Urban Heat Island (CUHI) effects, which are more directly linked to human thermal comfort and health. Incorporating in-situ observations from ground stations and mobile surveys would enhance the accuracy and validation of satellite-derived LST analyses. Integrating socio-economic and demographic data such as population density, income, and building characteristics can help identify heat-vulnerable zones and support equitable mitigation planning. Additionally, machine learning–based forecasting models and climate projection studies using CMIP6 scenarios can be developed to predict future UHI dynamics under varying urban growth and climate conditions. Such interdisciplinary approaches will aid in formulating climate-resilient urban planning and sustainable heat mitigation strategies for rapidly developing tropical cities like Coimbatore.

## ACKNOWLEDGMENTS

The authors also wish to thank the U.S. Geological Survey (USGS) for making available the satellite data. The authors wish to thank the anonymous reviewers for their constructive comments to enhance the quality of the manuscript.

## CONFLICT OF INTEREST

The authors declare that they have no competing interests.

## REFERENCES

Aghazadeh, F., Rahimi, A., Tarashkar, M., Firozjaei, M.K., Ioja, C., Ondrejicka, V., & Finka, M. (2025). *Assessing the Green Infrastructure and Built Up effects in Enhancing Thermal Comfort for Vulnerable Populations in Urban Heat Waves: A Case Study of Tabriz Metropolitan*. Remote Sensing Applications: Society and Environment, 101671.

Aher, M.C., & Yadav, S.M. (2021). Assessment of rainfall trend and variability of semi-arid regions of Upper and Middle Godavari basin, India. *Journal of Water and Climate Change*, 12(8), 3992-4006.

Arunab, K.S., & Mathew, A. (2023). Geospatial and statistical analysis of urban heat islands and thermally vulnerable zones in Bangalore and Hyderabad cities in India. *Remote Sensing Applications: Society and Environment*, 32, 101049. https://doi.org/10.1016/j.rsase.2023.101049.

Arunab, K.S., & Mathew, A. (2024). Quantifying urban heat island and pollutant nexus: A novel geospatial approach. *Sustainable Cities and Society*, 101, 105117. https://doi.org/10.1016/j.scs.2023.105117.

Badugu, A., Arunab, K.S., Mathew, A., & Sarwesh, P. (2023). Spatial and temporal analysis of urban heat island effect over Tiruchirappalli city using geospatial techniques. *Geodesy and Geodynamics,* 14(3), 275-291. https://doi.org/10.1016/j.geog.2022.10.004.

Directorate of Census Operations, Tamil Nadu. (2011). *Census of India 2011: Coimbatore District Census Handbook***.** Government of India. Retrieved from https://www.tnrd.tn.gov.in/databases/census_of_india_2011TN/pdf/13-Coimbatore.pdf

Chakraborty, T., & Lee, X. (2019). A simplified urban-extent algorithm to characterize surface urban heat islands on a global scale and examine vegetation control on their spatiotemporal variability. *International Journal of Applied Earth Observation and Geoinformation*, 74, 269-280. https://doi.org/10.1016/j.jag.2018.09.015.

Cheval, S., Amihăesei, V.A., Chitu, Z., Dumitrescu, A., Falcescu, V., Irașoc, A., ... & Tudose, N.C. (2024). A systematic review of urban heat island and heat waves research (1991–2022). *Climate Risk Management*, 44, 100603.

Coimbatore City Municipal Corporation. (2006). *City Development Plan* [Report]. Coimbatore City Municipal Corporation. Retrieved from https://ccmc.gov.in/images/stories/CDP/City_Development_Plan.pdf

da Silva Lopes, E., & Hora, K.E.R. (2024). Impact of urban morphology on the intensity of nocturnal heat islands: Analysis through the validation of simulation models in central-west Brazil. *Urban Climate*, 56, 102047. https://doi.org/10.1016/j.uclim.2024.102047.

Das, J., Mandal, T., & Saha, P. (2019). Spatio-temporal trend and change point detection of winter temperature of North Bengal, India. *Spatial Information Research*, 27(4), 411-424.

Dewan, A., Kiselev, G., & Botje, D. (2021). Diurnal and seasonal trends and associated determinants of surface urban heat islands in large Bangladesh cities. *Applied Geography*, 135, 102533.

Friedl, M.A., Sulla-Menashe, D., Tan, B., Schneider, A., Ramankutty, N., Sibley, A., & Huang, X. (2010). MODIS Collection 5 global land cover: Algorithm refinements and characterization of new datasets. *Remote sensing of Environment*, 114(1), 168-182.

Grigoraş, G., & Uriţescu, B. (2018). Spatial hotspot analysis of Bucharest's urban heat island (UHI) using modis data. Annals of Valahia University of Targoviste. *Geographical Series*, 18(1), 14-22. DOI: 10.2478/avutgs-2018-0002.

Grimm, N.B., Faeth, S.H., Golubiewski, N.E., Redman, C.L., Wu, J., Bai, X., & Briggs, J.M. (2008). Global change and the ecology of cities. *Science*, 319(5864), 756-760. https://doi.org/10.1126/science.1150195.

Grover, A., & Singh, R.B. (2015). Analysis of urban heat island (UHI) in relation to normalized difference vegetation index (NDVI): A comparative study of Delhi and Mumbai. *Environments*, 2(2), 125-138. https://doi.org/10.3390/environments2020125.

Guerri, G., Crisci, A., Messeri, A., Congedo, L., Munafò, M., & Morabito, M. (2021). Thermal summer diurnal hot-spot analysis: The role of local urban features layers. *Remote Sensing*, 13(3), 538.

Gupta, N., Mathew, A., & Khandelwal, S. (2020). Spatio-temporal impact assessment of land use/land cover (LU-LC) change on land surface temperatures over Jaipur city in India. *International Journal of Urban Sustainable Development,* 12(3), 283-299.

Halder, B., Chatterjee, P., Rana, B., Bandyopadhyay, J., Pande, C.B., Ahmed, K.O., ... & Radwan, N. (2024). Delineating the climate change impacts on urban environment along with heat stress in the Indian tropical city. *Physics and Chemistry of the Earth, Parts A/B/C*, 136, 103745. https://doi.org/10.1016/j.pce.2024.103745.

Hao, M., Liu, X., & Li, X. (2025). Quantifying heat-related risks from urban heat island effects: A global urban expansion perspective. *International Journal of Applied Earth Observation and Geoinformation,* 136, 104344. https://doi.org/10.1016/j.jag.2024.104344.

Harlan, S.L., Brazel, A.J., Prashad, L., Stefanov, W.L., & Larsen, L. (2006). Neighborhood microclimates and vulnerability to heat stress. *Social science & medicine*, 63(11), 2847-2863.

Jain, S., Sannigrahi, S., Sen, S., Bhatt, S., Chakraborti, S., & Rahmat, S. (2020). Urban heat island intensity and its mitigation strategies in the fast-growing urban area. *Journal of Urban Management,* 9(1), 54-66. https://doi.org/10.1016/j.jum.2019.09.004.

Kara, Y., Yavuz, V., & Lupo, A.R. (2025). Multi-Index Assessment of Surface Urban Heat Island (SUHI) Dynamics in Samsun Using Google Earth Engine. *Atmosphere*, 16(6), 712.

Kendall, M.G. (1938). A new measure of rank correlation. *Biometrika*, 30(1-2), 81-93. https://doi.org/10.1093/biomet/30.1-2.81.

Khandelwal, S., Goyal, R., Kaul, N., & Mathew, A. (2018). Assessment of land surface temperature variation due to change in elevation of area surrounding Jaipur, India. The Egyptian *Journal of Remote Sensing and Space Science*, 21(1), 87-94. https://doi.org/10.1016/j.ejrs.2017.01.005.

Kikon, N., Singh, P., Singh, S.K., & Vyas, A. (2016). Assessment of urban heat islands (UHI) of Noida City, India using multi-temporal satellite data. *Sustainable Cities and Society*, 22, 19–28. https://doi.org/10.1016/j.scs.2016.01.005.

Kim, J., Yeom, S., & Hong, T. (2025). Analyzing the cooling effect, thermal comfort, and energy consumption of integrated arrangement of high-rise buildings and green spaces on

urban heat island. *Sustainable Cities and Society*, 119, 106105. https://doi.org/10.1016/j.scs.2024.106105.

Li, J., Song, C., Cao, L., Zhu, F., Meng, X., & Wu, J. (2011). Impacts of landscape structure on surface urban heat islands: A case study of Shanghai, China. *Remote sensing of environment*, 115(12), 3249-3263. https://doi.org/10.1016/j.rse.2011.07.008.

Liu, Z., & Zhang, S. (2025). Exploring the relationship between urban green development and heat island effect within the Yangtze River Delta Urban Agglomeration. *Sustainable Cities and Society*, 106204. https://doi.org/10.1016/j.scs.2025.106204.

Mahajan, D.R., & Dodamani, B.M. (2015). Trend analysis of drought events over upper Krishna basin in Maharashtra. *Aquatic Procedia*, 4, 1250-1257.

Mahata, B., Sahu, S.S., Sardar, A., Laxmikanta, R., & Maity, M. (2024). Spatiotemporal dynamics of land use/land cover (LULC) changes and its impact on land surface temperature: a case study in new town Kolkata, eastern India. *Regional Sustainability*, 5(2), 100138. https://doi.org/10.1016/j.regsus.2024.100138.

Mathew, A., Arunab, K.S., & Sharma, A.K. (2024). Revealing the urban heat Island: Investigating spatiotemporal surface temperature dynamics, modeling, and interactions with controllable and non-controllable factors. *Remote Sensing Applications: Society and Environment*, 35, 101219. https://doi.org/10.1016/j.rsase.2024.101219.

Mathew, A., Khandelwal, S., & Kaul, N. (2016). Spatial and temporal variations of urban heat island effect and the effect of percentage impervious surface area and elevation on land surface temperature: Study of Chandigarh city, India. *Sustainable Cities and Society*, 26, 264-277.

Mathew, A., Khandelwal, S., & Kaul, N. (2017). Investigating spatial and seasonal variations of urban heat island effect over Jaipur city and its relationship with vegetation, urbanization and elevation parameters. *Sustainable cities and society*, 35, 157-177. https://doi.org/10.1016/j.scs.2017.07.013.

Mathew, A., Khandelwal, S., & Kaul, N. (2018). Analysis of diurnal surface temperature variations for the assessment of surface urban heat island effect over Indian cities. *Energy and Buildings*, 159, 271–295. https://doi.org/10.1016/j.enbuild.2017.10.062.

Mathew, A., Sarwesh, P., & Khandelwal, S. (2022). Investigating the contrast diurnal relationship of land surface temperatures with various surface parameters represent vegetation, soil, water, and urbanization over Ahmedabad city in India. *Energy Nexus*, 5, 100044.

Mavrakou, T., Polydoros, A., Cartalis, C., & Santamouris, M. (2018). Recognition of thermal hot and cold spots in urban areas in support of mitigation plans to counteract overheating: application for Athens. *Climate*, 6(1), 16.

Mohammad, P., & Goswami, A. (2021). Quantifying diurnal and seasonal variation of surface urban heat island intensity and its associated determinants across different climatic zones over Indian cities. *GIScience & Remote Sensing*, 58(7), 955-981.

Mohan, M., Kikegawa, Y., Gurjar, B.R., Bhati, S., & Kolli, N.R. (2013). Assessment of urban heat island effect for different land use–land cover from micrometeorological measurements and remote sensing data for megacity Delhi. *Theoretical and applied climatology*, 112, 647-658.https://doi.org/10.1007/s00704-012-0758-z.

Mora, C., Dousset, B., Caldwell, I.R., Powell, F.E., Geronimo, R.C., Bielecki, C.R., ... & Trauernicht, C. (2017). Global risk of deadly heat. *Nature climate change*, 7(7), 501-506.

Ngarambe, J., Oh, J.W., Su, M.A., Santamouris, M., & Yun, G.Y. (2021). Influences of wind speed, sky conditions, land use and land cover characteristics on the magnitude of the urban heat island in Seoul: An exploratory analysis. *Sustainable Cities and Society*, 71, 102953.

Oke, T.R. (1982). The energetic basis of the urban heat island. *Quarterly Journal of the Royal Meteorological Society,* 108(455), 1-24.

Ord, J.K., & Getis, A. (1995). Local spatial autocorrelation statistics: distributional issues and an application. *Geographical analysis*, 27(4), 286-306. https://doi.org/10.1111/j.1538-4632.1995.tb00912.x.

Pandey, A.K., Singh, S., Berwal, S., Kumar, D., Pandey, P., Prakash, A., ... & Kumar, K. (2014). Spatio–temporal variations of urban heat island over Delhi. *Urban Climate*, 10, 119-133. https://doi.org/10.1016/j.uclim.2014.10.005.

Pandey, A., Mondal, A., & Guha, S. (2024). Assess the relationship of land surface temperature with nine land surface indices in a northeast Indian city using summer and winter Landsat 8 data. *Cogent Engineering*, 11(1), 2382885. https://doi.org/10.1080/23311916.2024.2382885.

Patriota, E.G., Bertrand, G.F., Almeida, C.D.N., Claudino, C.M.D.A., & Coelho, V.H.R. (2024). Heat the road again! Twenty years of surface urban heat island intensity (SUHII) evolution and forcings in 21 tropical metropolitan regions in Brazil from remote sensing analyses. *Sustainable Cities and Society*, 113, 105629. https://doi.org/10.1016/j.scs.2024.105629.

Peel, M.C., Finlayson, B.L., & McMahon, T.A. (2007). Updated world map of the Köppen-Geiger climate classification. *Hydrology and earth system sciences*, 11(5), 1633-1644.

Peng, S., Piao, S., Ciais, P., Friedlingstein, P., Ottle, C., Bréon, F. M., ... & Myneni, R. B. (2012). Surface urban heat island across 419 global big cities. *Environmental science & technology*, 46(2), 696-703. https://pubs.acs.org/doi/full/10.1021/es2030438.

Peng, W., Yang, X., & Chen, S.S. (2024). Effect of the reference rural landscape on annual variations in surface urban heat island intensity. *Sustainable Cities and Society*, 115, 105804. https://doi.org/10.1016/j.scs.2024.105804.

Puttanapong, N., Nuengjumnong, N., SaeJung, J., & Moukomla, S. (2025). A 36-year geospatial analysis of urbanization dynamics and surface urban heat island effect: Case study of the Bangkok Metropolitan Region. *Geography and Sustainability*, 6(4), 100322.

Radoux, J., Dominique, M., Hartley, A., Lamarche, C., Bos, A., & Defourny, P. (2025). Land Cover Types Drive the Surface Temperature for Upscaling Surface Urban Heat Islands with Daylight Images. *Remote Sensing*, 17(16), 2815.

Raj, S., & Yun, G.Y. (2025). Exploring the role of strategic urban planning and greening in decreasing surface urban heat island intensity. *Journal of Asian Architecture and Building Engineering*, 24(2), 866-879.

Ramachandra, T. V., Setturu, B., & Dey, M (2019). Land surface temperature responses to land use dynamics across the agro-climatic zones of Karnataka. Retrieved May 15, 2025, from https://www.bspublications.net/9789395038232/10.37285/bsp.ic2uhi.38.pdf.

Ramanathan, S.P., & Kokilavani, S. (2021). Comparison of the Monthly and Seasonal Estimates of Potential Evapotranspiration for Coimbatore Station of Tamilnadu Using Different Methods. *Mausam*, 72(3), 681-684.

Rizwan, A.M., Dennis, L.Y., & Liu, C. (2008). A review on the generation, determination and mitigation of Urban Heat Island (UHI). *Journal of Environmental Sciences*, 20(1), 120-128. https://doi.org/10.1016/S1001-0742(08)60019-4.

Rossi, F., & Becker, G. (2019). Creating forest management units with Hot Spot Analysis (Getis-Ord Gi*) over a forest affected by mixed-severity fires. *Australian Forestry*, 82(4), 166-175. https://doi.org/10.1080/00049158.2019.1678714.

Sahana, M., Sajjad, H., & Ahmed, R. (2018). Analyzing urban expansion and land surface temperature changes in Chennai City using geospatial techniques. *Geocarto International*, 33(4), 414–432. https://doi.org/10.1016/j.scitotenv.2018.02.170.

Santamouris, M. (2015). Analyzing the heat island magnitude and characteristics in one hundred Asian and Australian cities and regions. *Science of the Total Environment*, 512–513, 582–598. https://doi.org/10.1016/j.scitotenv.2015.01.060.

Sen, P.K. (1968). Estimates of the regression coefficient based on Kendall's tau. *Journal of the American statistical association,* 63(324), 1379-1389. https://doi/abs/10.1080/01621459.1968.10480934.

Shahfahad, Talukdar, S., Rihan, M., Hang, H.T., Bhaskaran, S., & Rahman, A. (2021). Modelling urban heat island (UHI) and thermal field variation and their relationship with land use indices over Delhi and Mumbai metro cities. *Environment, Development and Sustainability*, 1-29. https://doi.org/10.1007/s10668-021-01587-7.

Sharma, R., & Joshi, P. K. (2013). Monitoring urban landscape dynamics over Delhi (India) using remote sensing (1998–2011) inputs. *Journal of the Indian Society of Remote Sensing*, 41(3), 641-650.

Tan, J., Zheng, Y., Tang, X., Guo, C., Li, L., Song, G., ... & Chen, H. (2010). The urban heat island and its impact on heat waves and human health in Shanghai. *International journal of biometeorology*, 54(1), 75-84.

Tong, S., Prior, J., McGregor, G., Shi, X., & Kinney, P. (2021). Urban heat: an increasing threat to global health. bmj, 375.

Voogt, J. (2007, July). How researchers measure urban heat islands. In *United States Environmental Protection Agency (EPA)*, State and Local Climate and Energy Program, Heat Island Effect, Urban Heat Island Webcasts and Conference Calls.

Voogt, J.A., & Oke, T.R. (2003). Thermal remote sensing of urban climates. *Remote Sensing of Environment,* 86(3), 370-384. https://doi.org/10.1016/S0034-4257(03)00079-8.

Wan, Z., Hook, S., & Hulley, G. (2015). *MOD11A2 MODIS/Terra Land Surface Temperature/Emissivity 8-Day L3 Global 1km SIN Grid V006* [Data set]. NASA Land Processes Distributed Active Archive Center. https://doi.org/10.5067/MODIS/MOD11A2.006 Date Accessed: 2025-10-29.

Wang, C., & Chang, H.T. (2020). Hotspots, heat vulnerability and urban heat islands: An Interdisciplinary Review of Research Methodologies. *Canadian Journal of Remote Sensing*, 46(5), 532-551. https://doi.org/10.1080/07038992.2020.1816815

Wang, J., Lu, L., Zhou, X., Huang, G., & Chen, Z. (2025). Spatio-Temporal patterns and drivers of the urban heat island effect in arid and semi-arid regions of Northern China. *Remote Sensing*, 17(8), 1339.

Wang, J., Zhou, W., & Zhao, W. (2023). Higher UHI intensity, higher urban temperature? A synthetical analysis of urban heat environment in urban megaregion. *Remote Sensing*, 15(24), 5696.

Wang, X., Wang, J., Yao, J., Niu, J., & Hou, Y. (2025a). *Driving mechanism of urban heat*

*island spread in the Central-Southern Liaoning Urban Agglomerations, China (2013–2020).* Environmental and Sustainability Indicators, 100962.

Wang, J., Lu, L., Zhou, X., Huang, G., & Chen, Z. (2025b). Spatio-temporal patterns and drivers of the urban heat island effect in arid and semi-arid regions of Northern China. *Remote Sensing*, 17(8), 1339.

Weng, Q., Lu, D., & Schubring, J. (2004). Estimation of land surface temperature–vegetation abundance relationship for urban heat island studies. *Remote Sensing of Environment*, 89(4), 467–483. https://doi.org/10.1016/j.rse.2003.11.005.

Wu, Q., Huang, Y., Irga, P., Kumar, P., Li, W., Wei, W., ... & Zhou, J. L. (2024). Synergistic control of urban heat island and urban pollution island effects using green infrastructure. *Journal of Environmental Management*, 370, 122985.

Xiong, X., Angal, A., Chang, T., Chiang, K., Lei, N., Li, Y., ... & Wu, A. (2020). MODIS and VIIRS calibration and characterization in support of producing long-term high-quality data products. *Remote Sensing*, 12(19), 3167.

Zhang, Y., Xie, M., Chen, Y., Deng, Q., Zhao, X., & Chen, Y. (2025). Spatiotemporal evolution of the regional heat island effect and its influencing factors in the Beijing–Tianjin–Hebei urban agglomeration. Remote Sensing Applications: *Society and Environment*, 101749.

Zhao, L., Lee, X., Smith, R.B., & Oleson, K. (2014). Strong contributions of local background climate to urban heat islands. *Nature*, 511(7508), 216–219. https://doi.org/10.1038/nature13462.

Zhou, D., Zhao, S., Zhang, L., Sun, G., & Liu, Y. (2015). The footprint of urban heat island effect in China. *Scientific reports*, 5(1), 11160.

Zwolska, A., Półrolniczak, M., & Kolendowicz, L. (2025). Remote sensing-based analysis of urban land cover changes and surface urban heat island dynamics using Landsat and Local Climate Zones classification in Poznań, Poland. IEEE Journal of Selected Topics in Applied Earth Observations and Remote Sensing.